

148ⁿ

SATELLITE DATA APPLIED TO HYDROLOGIC MODELS FOR REGIONAL
WATERSHEDS: A CASE STUDY, APURE LLANOS, VENEZUELA

by
Rafael Lairer C. (Lic.)

A Research Report
Submitted to the School of Graduate Studies
in Partial Fulfilment of the Requirements
for the Degree
Master of Arts

McMaster University
September, 1977

MASTER OF ARTS (1977)

McMASTER UNIVERSITY
Hamilton, Ontario

TITLE: Satellite Data Applied to Hydrologic Models for Regional
Watersheds: A Case Study, Apure Llanos, Venezuela.

AUTHOR: Rafael Lairet C. (Licenciate in Geography
Universidad Central de Venezuela)

SUPERVISOR: Dr. Philip J. Howarth

NUMBER OF PAGES: x, 105

ABSTRACT

Satellite data from GOES and LANDSAT were evaluated as a source of information for hydrologic distributed models applied to large watersheds. Three basins within the Llanos area of the Orinoco River basin, Venezuela, were selected as study areas.

The specific objectives of the study were:

- (1) To test the applicability of meteorological satellite data for improving information on the temporal and areal distribution of precipitation, as well as estimates of amount over large areas.
- (2) To investigate photographic and digital LANDSAT data as a source of land surface information for hydrologic distributed models.

The satellite and ground data used in this research were:

- (1) GOES WEFAX electrostatic facsimiles,
- (2) LANDSAT photographic and digital data,
- (3) Reports and maps on soil studies by Desarrollo Industrial Agricola C.A (1958) and Comerma and Luque (1971).

The analysis of the data was carried out by visual analysis on the photographic products of GOES and LANDSAT using regular photo-interpretation techniques. GOES photographic data allowed the analysis of temporal and areal distribution of precipitation over large areas. Follansbe's (1973) method for estimating precipitation using satellite imagery was found potentially applicable to hydrologic distributed

models. Variations to the method are suggested.

The visual analysis of a single LANDSAT image allowed the mapping of broad land-cover classes and some soil characteristics in the study area. Analysis of the multirate imagery was found very useful in detecting seasonal and non-seasonal changes.

Digital analysis of LANDSAT data was carried out on the Image 100 system at the Canada Centre for Remote Sensing in Ottawa. Contrast stretched images and breakpoint enhancement, supervised and unsupervised classifications were produced. The results showed that LANDSAT digital analysis either by unsupervised or supervised classification can be used for the extraction of land-use/land-cover information for application in hydrologic distributed models.

ACKNOWLEDGMENTS

The author is indebted to his supervisor Dr. Philip J. Howarth for his direction and enthusiasm for the project; to Dr. M. K. Woo for his comments and valuable suggestions; to Mr. Edgar Diaz Z. and Mr. Soler Rodriguez for their help in the gathering of the basic cartographic data for this research; to Dr. J.A. Comerma for providing invaluable information about the study area; to Eng^O Carlos Borges for supplying the basic hydrometeorological data; to Dr. Adolfo C. Romero and Dr. Alberto Rodriguez D. for their encouragement and interest for the project.

Particular thanks are due to the Canada Centre for Remote Sensing for allowing me to use the General Electric Image 100 System, to Mr. William Bruce and Mr. V.K. Potdar for their valuable help during the digital analysis process. Also thanks are due to the Ontario Centre for Remote Sensing whose Density Slicer equipment was used in this research as well as its GOES-1 data archives.

Finally, I would like to very deeply thank my wife Janet for her cooperation during all stages of the work, and especially for typing this paper; and to my daughter, Janet Angélica, always willing to help; and to the Fundacion Gran Mariscal de Ayacucho for its financial support.

TABLE OF CONTENTS

| | PAGE |
|-----------------|---|
| ABSTRACT | ii |
| ACKNOWLEDGMENTS | iv |
| LIST OF TABLES | vii |
| LIST OF FIGURES | viii |
| | |
| CHAPTER ONE | INTRODUCTION |
| | 1 |
| | 1.1 Statement of the Problem |
| | 1 |
| | 1.2 Objectives of the Present Study |
| | 2 |
| | 1.3 Outline of the Project |
| | 2 |
| CHAPTER TWO | REMOTE SENSING APPLICATIONS IN HYDROLOGIC MODELS: A LITERATURE REVIEW |
| | 4 |
| | 2.1 Introduction |
| | 4 |
| | 2.2 Hydrologic Mathematical Models |
| | 4 |
| | 2.3 Remote Sensing of Information for Mathematical Hydrologic Models. |
| | 8 |
| | 2.3.1 Hydrometeorologic Information |
| | 11 |
| | 2.3.2 Drainage Basin Characteristics |
| | 13 |
| | 2.4 Remote Sensing Applications to Hydrologic Models. |
| | 19 |
| CHAPTER THREE | STUDY AREA AND DATA |
| | 22 |
| | 3.1 Introduction |
| | 22 |
| | 3.2 Study Area |
| | 22 |
| | 3.3 Remote-Sensing Data |
| | 37 |
| | 3.4 Ground Data |
| | 41 |

| | | |
|--------------|---|-----|
| CHAPTER FOUR | APPLICATION OF GOES-1 DATA TO HYDROLOGIC DISTRIBUTED MODELS | 42 |
| | 4.1 Introduction | 42 |
| | 4.2 Analysis of GOES-1 Data | 42 |
| | 4.2.1 Analysis of Temporal and Areal Distribution of Precipitation based on GOES-1 data | 44 |
| | 4.2.2 Precipitation Estimates Using GOES-1 Imagery | 47 |
| | 4.3 Discussion | 52 |
| CHAPTER FIVE | EVALUATION OF LANDSAT DATA | 55 |
| | 5.1 Introduction | 55 |
| | 5.2 Visual Analysis | 57 |
| | 5.2.1 Introduction | 57 |
| | 5.2.2 Visual Analysis of Single Date Image | 58 |
| | 5.2.3 LANDSAT Temporal Analysis | 63 |
| | 5.3 Digital Analysis of LANDSAT Data | 70 |
| | 5.3.1 Systems for Analysing Digital Data | 70 |
| | 5.3.2 Digital Analysis Procedures | 74 |
| | 5.4 Discussion | 85 |
| CHAPTER SIX | CONCLUSIONS | 97 |
| BIBLIOGRAPHY | | 100 |
| APPENDIX A | Land-Use/Land-Cover Classification. | 104 |

LIST OF TABLES

| TABLE | | PAGE |
|-------|---|------|
| 2.I | Deterministic Models | 6 |
| 2.II | Classification of Data for Deterministic Models | 9 |
| 3.I | Landscapes, soil types, vegetation and drainage conditions in the study area. | 35 |
| 4.I | Formats of GOES-1 (75° W, 00°). | 43 |
| 4.II | GOES-1 Imagery recorded on June 10 1977. | 48 |
| 5.I | Image 100 Characteristics. | 72 |
| 5.II | Proportion of each theme displayed in the four study areas (MAT-1, MAT-2, MAT-3 and MAT-4) and the total scene. | 83 |
| 5.III | Vegetative Parameter "A" in Holtan Infiltration Equation (Land-Cover Types Found on the Study Area) | 89 |

LIST OF FIGURES

| FIGURE | | PAGE |
|--------|--|------|
| 3.1 | Location of the Venezuelan Llanos and Study Area. | 23 |
| 3.2 | General geologic map of the Study Area. | 25 |
| 3.3 | Apure Llanos: land districts and location of selected basins. | 26 |
| 3.4 | Cinaruco River basin map. | 28 |
| 3.5 | Capanaparo River basin map. | 29 |
| 3.6 | Matiyure River basin map. | 30 |
| 3.7 | Location of meteorological stations. | 31 |
| 3.8 | Monthly precipitation for Cararabo and Puerto Páez. | 33 |
| 3.9 | Monthly precipitation for San Fernando Apure and Corozo Pando. | 34 |
| 3.10 | General soil map of the study area. | 36 |
| 3.11 | Venezuelan Llanos: vegetation regions. | 38 |
| 4.1 | GOES-1 image of the visible spectral band (WC-1). | 45 |
| 4.2 | GOES-1 image of the thermal infrared spectral band. | 46 |
| 4.3 | GOES-1 image sequence taken on June 10 th 1977. | 49 |
| 4.4 | GOES-1 image of the visible band showing the grid element, and cloud clusters. | 54 |
| 5.1 | LANDSAT coverage of the study area. | 56 |
| 5.2 | Visual interpretation of LANDSAT image. | 60 |
| 5.3 | Soil interpretation using LANDSAT. | 62 |

| | | |
|------|---|------|
| 5.4 | Soil map of the study area. | 63 a |
| 5.5 | Visual interpretation of image taken on March 10 1973 | 64 |
| 5.6 | Variation in surface water bodies. | 66 |
| 5.7 | Density slicing of LANDSAT image: Case A | 68 |
| 5.8 | Density slicing of LANDSAT image: Case B | 69 |
| 5.9 | Location of the test areas: MAT-1, MAT-2, MAT-3 and MAT-4. | 71 |
| 5.10 | Image 100 system. | 73 |
| 5.11 | Breakpoint enhancement technique;Gould Printer output. | 75 |
| 5.12 | Colour composite of Bands 4,5 and 7 displayed on the CRT of the IMAGE 100. | 76 |
| 5.13 | Colour composite of Bands 4 and 5 stretched and normal Band 7 produced by the IMAGE 100 (CRT). | 77 |
| 5.14 | Unsupervised classification for MAT-1 test area. | 79 |
| 5.15 | Final unsupervised classification produced via EBIR for MAT-1 test area. | 81 |
| 5.16 | Final unsupervised classification produced via EBIR for MAT-3 test area, using signatures file created on MAT-1 | 82 |
| 5.17 | Final unsupervised classification produced via EBIR for the LANDSAT scene E-2029- 14142 | 84 |
| 5.18 | Final supervised classification produced via EBIR for MAT-1 test area. | 86 |
| 5.19 | Gould Printer scaled 1:100,000. A theme output of part of MAT-1,unsupervised classification (Forest). | 90 |
| 5.20 | Gould Printer unscaled. Themes output of part of MAT-1,unsupervised classification.(Forest) | 91 |
| 5.21 | Line Printer scaled 1:100,000. Themes output of part of MAT-1,unsupervised classification.(Forest). | 92 |
| 5.22 | Comparison between Gould Printer and Line Printer scaled 1:100,000 outputs. | 93 |

| | | |
|------|---|----|
| 5.23 | Comparison between Line Printer output and 1:100,000 scale topographic map. | 94 |
| 5.24 | Line Printer scaled 1:500,000. Themes output of scene displayed in Fig. 5.21 is outlined. | 95 |

CHAPTER 1

INTRODUCTION

1.1 Statement of the Problem

In recent years, the development and use of mathematical hydrologic models has increased greatly. Although there are many different types of models, they generally require a large amount of information. This information is obtained from climatologic and hydrologic records, from maps and aerial photographs and from field work. Ragan and Jackson (1975) pointed out that very often most of the time is spent on the information-gathering process, rather than on the running of the model and the interpretation of results.

The data-gathering process is obviously a great challenge when large drainage basins are involved. In such areas basic hydrometeorological data are usually scarce to non-existent. In addition to the size of the basins, seasonal variations in vegetation cover, surface runoff, the area of surface water and soil moisture content provide severe constraints on the use of conventional data sources such as aerial photography and topographic maps. There is usually a lack of data with regard to geology, soils and vegetation types and cover. All these factors cause difficulties, not only for hydrologic response modelling, but also for watershed management.

Remote sensing from spacecraft such as SMS-GOES and LANDSAT provides a possible means of gathering part of the information rapidly,

economically, repetitively and with an acceptable accuracy. To maximize the potential benefit of remote sensing for large drainage basin studies, the values and limitations of this approach must be understood.

1.2 Objectives of the Study

The specific objectives of this research are:

- (1) To test the applicability of meteorological satellites (SMS-GOES) for improving the information on the areal distribution of precipitation. The application of that information to deterministic hydrologic models will also be considered.
- (2) To evaluate the methods for estimating the amount of precipitation from satellite data.
- (3) To investigate photographic and digital LANDSAT data as a source of land surface information.
- (4) To study the possibilities of using information from satellite data as an input for deterministic distributed models.

1.3 Outline of the Project

In this chapter the statement of the problem and the objectives of the study have been presented. The following chapters are related to an evaluation of remotely-sensed data as a source of information for hydrologic mathematical models.

Chapter 2 is devoted to a review of the literature on this subject. In the first part, the concept, purposes and the types of models

able to receive information from remote sensing are presented. In the second part, the fundamental principles involved in remote sensing of physical properties of objects and media are discussed. This provides a base for the direct and indirect extraction of information applicable to hydrologic models. In the third part, comments are presented regarding the literature on remote sensing in watershed modelling.

The study area and the data used in this research are presented in Chapter 3.

The evaluation of GOES data as a source of information for precipitation inputs (areal distribution and estimates of amount) to distributed models is presented in Chapter 4.

In Chapter 5, the results of the evaluation of LANDSAT as a source of information on drainage basin characteristics (physiography, land use/land cover and soil) is presented. The possibility of using such information as an input to hydrologic deterministic distributed model is discussed.

In Chapter 6 the conclusions of this research are presented.

CHAPTER 2

REMOTE SENSING APPLICATIONS IN HYDROLOGIC MODELS: A LITERATURE REVIEW.

2.1 Introduction.

This review is divided into three parts. First it is necessary to analyze the concept of hydrologic models, their purpose and which of them are capable of receiving information extracted from remotely-sensed data. Second, how information applicable to hydrologic deterministic models is gathered by means of remote-sensing systems must be considered. Finally, one must examine the work already carried out by other authors dealing with remote-sensing applications to hydrologic mathematical models.

2.2 Hydrologic Mathematical Models.

Based on a general definition of mathematical models given by Weik (1969), a hydrologic mathematical model may be defined as a mathematical representation of an hydrologic process, which allows mathematical manipulations of variables as a means of determining how the process reacts in different situations or under different stimuli.

Freeze (1974) holds that a general form of a hydrologic model can be expressed as:

$$y_t = f(x_{t-1}, x_{t-2}, \dots, y_{t-1}, y_{t-2}, \dots, a_1, a_2, \dots) + \epsilon_t \quad (1)$$

where:

x_t = represents the input at time t

y_t = corresponds to the output at time t

a = the system parameters

f = defines the model function

ϵ = expresses the error or lack of fit of the model with reality.

Mathematical models in hydrology have been in use since the early sixties. A better understanding of various hydrologic process has aided their development. Also of importance has been the availability of digital computers that allow the manipulation of large amounts of hydrologic and meteorologic data at high speed.

At present, very little can be added by remote sensing to stochastic and streamflow routing models. It is in the realm of the deterministic conceptual models¹ where remote sensing could have its most valuable contribution

In Table 2.1, a list of some of the commonly used deterministic models is presented. It can be observed that the majority of these models are lumped, and only a few of them are partially or totally distributed. The main difference between them is one of spatial or temporal averaging. A lumped model is one in which the basin is considered as a single entity and the model parameters represent an average value for the entire basin. In the distributed models, the basin is sub-divided into a finite

(¹) " If all variables in equation (1) are regarded as free from random variations, so that none is thought of as having a distribution in probability, then the model is regarded as deterministic"(Clarke, 1973, p. 3)

TABLE 2.1 DETERMINISTIC MODELS.

| <i>Date</i> | <i>Name of Model</i> | <i>Land Surface Parameter Representation</i> |
|-------------|---|--|
| 1958 | SSARR Corp. of Engineers Model | Lumped |
| 1959-1966 | Stanford Watershed Models | Lumped |
| 1962 | Road Research Laboratory Model | Lumped |
| 1965 | Dawdy and O'Donnell Model | Lumped |
| 1966 | Boughton Model | Lumped |
| 1966 | Huggins and Monke Model | Distributed |
| 1967 | Hydrocomp Simulation Program | Lumped |
| 1968 | Kutchment Model | Lumped |
| 1968 | Schultz Model | Distributed |
| 1968 | Hydrologic Engineering Center (US) Model | Lumped |
| 1969 | USDAHL-70 Agricultural Research Service Model | Lumped |
| 1969 | Kozak Model | Partly distributed |
| 1969 | Mero Model | Lumped |
| 1970 | Institute of Hydrology Model | Lumped |
| 1970 | Vemuri and Dracup Model | Lumped |
| 1971 | Van de Nes and Hendriks Model | Distributed |
| 1972 | Water Resources Board Dee Research Model | Lumped |
| 1974 | Gupta Model | Distributed |

After: Fleming (1975)

number of units. Calculations are carried out in each of these units, surface characteristics and climatological information being average values.

Several authors have pointed out the problems of lumping. Murray (1970) suggested that inaccuracies can be introduced into the simulation by lumping input such as precipitation in both space and time. The same problem occurs when assigning an averaged infiltration rate to the whole basin.

Freeze (1969) holds that the purposes of hydrologic response models are:

- (1) To synthesize past hydrologic events,
- (2) To predict future hydrologic events and to evaluate, for design purposes, combinations of hydrologic events occurring rarely in nature,
- (3) To evaluate the effects of artificial changes imposed by man on the hydrologic regime, and
- (4) To provide a mean of research for improving our understanding of hydrology in general, and the runoff process in particular.

If the model is to be used in analyzing the influence of temporal and spatial variations of climatologic inputs, as well as changes in basin characteristics (land use/land cover), a distributed approach is the most appropriate to use. This is of particular importance in urban, agricultural and forest hydrology.

The hydrologic distributed models operate on a grid element basis. Therefore the information (climatologic and land use/land cover

inputs) has to be gathered at the same level. It can be appreciated that the procedure is time-consuming, particularly when large basins are involved. This situation will become a problem if the information does not exist in the correct format for the model. Up to now the most suitable approach is by digitizing thematic maps or interpretations from photography. It has been suggested that remote-sensing systems such as SMS-GOES and LANDSAT could be used as sources of data for distributed climatologic inputs and drainage basin characteristics.

2.3 Remote Sensing of Information for Mathematical Hydrologic Models.

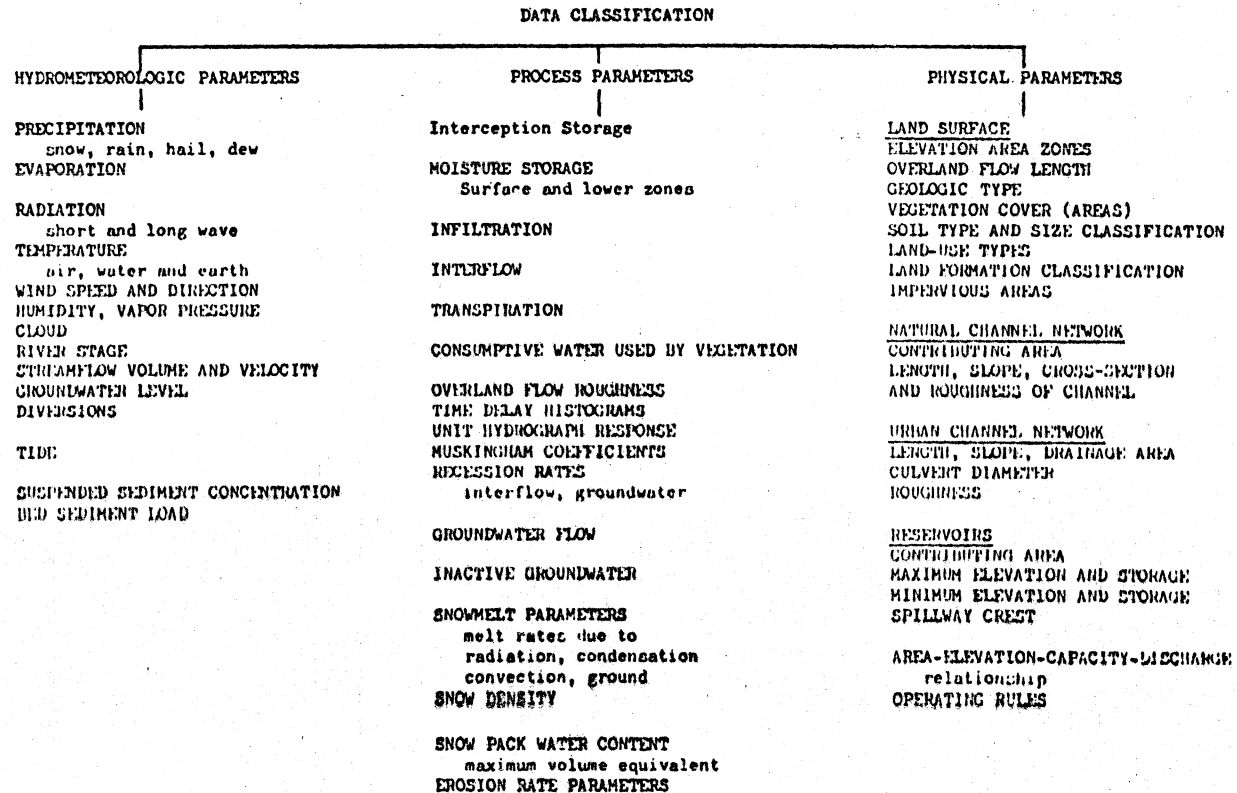
A classification of data normally required for deterministic hydrologic models (Fleming, 1975) is shown in Table 2.II. Information for hydrologic models can be extracted by remote-sensing techniques in three forms:

- (1) direct qualitatively,
- (2) direct quantitatively, and
- (3) indirect or by correlation between ground measurements and some properties of the remotely-sensed data
(Meyer and Welch, 1975).

In direct quantitative measurements, spatial resolution and radiometric fidelity are the most important factors. In the latter case, scene contrast affects the detection and therefore direct measurement.

The direct measurements involve the interaction between

TABLE 2.II CLASSIFICATION OF DATA FOR DETERMINISTIC MODELS.



Source: George Fleming, "Computer Simulation Techniques in Hydrology",
 (New York: Elsevier), 1975, p. 56

the electromagnetic radiation and the objects. The change suffered by the electromagnetic radiation when it is reflected, emitted, absorbed or transmitted by different objects are used as a source of information to analyze the properties of these objects.

The possibility of working in different spectral regions in which each one of these elements has its unique or characteristic spectral signature, allows their identification. By monitoring changes in the spectral response of water, soil, vegetation and clouds, seasonal variations, as well as changes in physical properties of those elements can be followed.

Several remote-sensing systems are capable of gathering information to be applied to distributed hydrological models. Conventional aerial photography (panchromatic, black and white infrared, colour and colour infrared) has been used for years and is considered the best system available. Radar, as well as multispectral scanners on aircraft, has been used to extract information potentially useful for hydrologic models. However, limitations imposed by the size of the basins and seasonal changes reduce the applicability of these systems.

Based on Table 2.II and considering the actual capabilities of the spaceborne sensors (SMS-GOES and LANDSAT), it seems feasible to gather the following information for hydrologic models:

- (1) Areal distribution and estimates of amount of precipitation.
- (2) Land surface data including land use/land cover and soil characteristics.

Therefore in the following sections a review of the literature dealing with the use of meteorological satellites and LANDSAT, in obtain-

ing that information, will be presented and discussed.

2.3.1 Hydrometeorological Information.

Since the first operational meteorological satellite system inaugurated by the launching of ESSA 1 in February 1966, great attention has been given to the interpretation of remotely-sensed data in terms of atmospheric parameters normally observed using conventional methods (Barrett, 1973). Precipitation is one of these parameters, and is without doubt the most important climatological input for hydrologic models.

Rain gauge networks are the most widely used system for measuring precipitation. They are generally dense in populated areas, but scarce (if not totally absent) in rural areas and in the remote and isolated upper portions of basins. Because of the areal variability of precipitation, the estimation of average rainfall over an area has always been a problem. Several methods have been developed to overcome this. Arithmetic mean, Thiessen polygons and Isohyetal procedures are the most widely used. All of them, however, are greatly affected by rain gauge distribution. This problem becomes critical when dealing with large and poorly instrumented basins, a very common situation in tropical countries. Because of the uneven distribution of the rain gauges, convectional storms (very localized and common phenomena in the Tropics) could occur and go unmeasured.

As was pointed out by Gruber (1973), for the measurement of the area covered by precipitation, satellite data are better than any data obtained from ground acquisition systems, with the exception of radar. It has been found, however, that radar systems are only suitable for measurements up to 100 n.mi. This is because for greater distances

the earth's curvature affects the measurement. Information from satellites thus becomes suitable to help solve the problem of precipitation distribution over large areas.

Martin and Sherer (1973) pointed out that satellite borne sensors do not see rain directly, neither do they respond selectively to rain and frozen drops, as does radar. Spatial resolution has also been mentioned as a limitation on the use of meteorological satellite data, since it does not permit the exact location of the cloud in relation to a geographical grid system.

In spite of these constraints, several methods have been developed to estimate rainfall from satellite data. Precipitation estimates have been obtained by analysis of cloud characteristics such as type, size and brightness, (Conover, 1962; Barrett, 1967). Barrett (1970) obtained a rainfall coefficient based on cloud cover and cloud type to estimate monthly precipitation. Follansbe (1973) improved Barrett's approach using satellite images instead of clouds charts and developed an equation for estimating daily rainfall. He only considered rain producing clouds, however, such as cumulonimbus, nimbostratus and cumulus congestus. This will be discussed further in Chapter 4.

Woodley and Sancho (1971) and Martin and Suomi (1972) found that cloud brightness correlates well with large radar echoes. This is based on the assumption that the brightest cloud masses on the satellite imagery will correspond to the clouds with the greatest vertical development. These clouds are the most likely ones to contain precipitation areas. Woodley and Sancho (1971) found that 87 % of the 372 radar echoes detected by the 10 cm. University of Miami's radar system fell

within brightness spots. It was also found that 70 % of 124 bright spots were related to radar echoes. They emphasized that changes of the cloud system with time seem to affect the rainfall estimate when using the brightness method.

There are still some limitations, however, to the use of satellite data in estimating precipitation. Martin and Sherer (1973) hold that for precipitation estimates of 24 hours or less over small areas, it is necessary that the cloud seen in the imagery be representative of or dominant for the period. Changes in time indeed affect estimates from satellite data, particularly those made using the brightness approach. It has been observed that the brightness approach tends to underestimate precipitation when cloud of low brightness produces significant rain, and conversely, it overestimates precipitation when bright clouds produce no significant rain.

Martin and Sherer (1973) point out that most methods concentrate on estimating convective rainfall. Therefore observations are required to isolate areas of convective activity from background cloudiness. It is also important to establish the effect of nonconvective rainfall on the area under study.

Better rainfall estimates can probably be obtained with developments such as spaceborne sensors working in the microwave region, as well as through improvements in spatial resolution, navigational accuracy and continuous coverage.

2.3.2 Drainage Basin Characteristics.

For modelling purposes and especially for distributed models, drainage basin characteristics are sub-divided into two groups. First

those derived from drainage basin physiographic characteristics including:

- (1) River basin boundary,
- (2) River basin area,
- (3) Grid element,
- (4) Channel network (stream length, stream order),
- (5) Topography (contour lines, elevation, average slope, aspect of slope, etc.), and
- (6) Flow paths and direction of the flow

The second group includes:

- (1) Land use/land cover and
- (2) Soil characteristics.

After: Gupta (1974)

Fleming (1975) holds that parameters derived from drainage basin characteristics are required in digital simulation because they are used to define the retention and release characteristics of the basin. He also mentioned that this information can be incorporated into equations for calculating the rate at which water moves from the land surface (Fleming, 1975).

Measurements of basin physiographic characteristics are possible using most remote-sensing imaging systems. The feasibility of observing and measuring these characteristics depends on a composite effect between the size of the feature and the resolving power of the system. Up to now, the type of information mentioned has normally been extracted from maps and aerial photography. These data sources are considered the best available.

Due to the characteristics of satellite borne sensors, it is not possible to measure parameters such as elevation, average slope and contour lines, within the range of precision required, although

with future development it may be possible. However, Kesik (1973) and Rango et al. (1975) found that LANDSAT imagery allows the detection and measurement of certain characteristics. These characteristics are drainage density, basin area, basin boundary and stream length. It has been suggested that LANDSAT could be used to extract information equivalent to that gathered from 1:1000,000 scale maps. In some cases, particularly in dissected terrain, information equivalent to 1:100,000 scale maps can be obtained. However, in areas with dense forest the amount of information that can be extracted is diminished by the masking effect of vegetation.

The second group, as was mentioned before, is formed by land use/land cover and soil information. The use of the term land use or land cover depends on the conditions of the area to be studied. In rural areas in which no use of the land is apparent, there is a tendency to consider the information extracted as land cover.

The amount of information required on land use/land cover will depend on the model under consideration. In his model, Gupta (1974) used a version of a land-use/land-cover classification based on the Canada Land Inventory. The classification is shown in Appendix A. In the model, the effects upon infiltration of each class ("A" parameter in Holtan, 1971 equation) is considered by assigning to each one of them a relative coefficient. For each grid element (5x5 km.) a weighted average coefficient is computed to account for the percentage of cover of each class.

As can be seen, information on land use/land cover is required in detail. Thus in the following sections a discussion will be presented

on how remote sensing has been used to detect and measure vegetation, water and soil characteristics.

Vegetation: vegetation has an important role in the hydrologic cycle. It controls processes such as evapotranspiration and infiltration. Structure and density are the most important elements in describing vegetation for application in hydrologic models. Vegetation structure refers to the separation of the different vegetational strata, such as tree, shrub, dwarf shrub and herb layers. Density may be defined as the percentage of vegetative cover in relation to the soil background.

Fleming (1975) proposed a general classification for vegetation types when zoning a drainage basin. They are:

- (1) Heavy forest,
- (2) Forested areas,
- (3) Mixed forest and openland,
- (4) Openland
 - a. Natural grassland
 - b. Agricultural grassland, and
- (5) Non vegetated areas (bare surface).

The separation of these classes is based on their differing effects upon the hydrologic processes already mentioned.

The effect of vegetation and changes in vegetation cover on basin hydrologic response have been demonstrated in the literature. These changes can be classified as seasonal and non-seasonal. The seasonal changes are expressed by variations in vegetation density rather than structural changes. Non-seasonal changes occur as a product of fire

damage or human activity.

Both changes affect spectral response of the vegetation. The influence of maturation, water content variations and senescence on spectral reflectance have been analyzed under laboratory conditions. A very extensive literature dealing with these aspects is covered in Myers (1975). In the same publication the principles involved in the detection of vegetation using remote sensing systems are discussed.

Several authors have demonstrated the possibilities of using LANDSAT data, either visual or digital, in studying the seasonal variations of vegetation. Structural changes resulting from fire damages have been detected and measured using LANDSAT data, as demonstrated by Deshler (1974) and Lauer and Krumpe (1973).

Detection and measurement of these changes can be performed using LANDSAT data. Measurement can be made using any conventional measuring device (planimeter or ruler, etc.) when using photographic products. More precise measurements, however, can be obtained using digital products. Area measurements using the pixel counting technique have been found useful in estimating, for example, vegetation cover and fire extension.

Quantitative estimates of spectral reflectance can be obtained using digital data allowing the monitoring of seasonal variations.

Water: The LANDSAT repetitive coverage permits the monitoring of seasonal variations in surface waters (lake, ponds). This is an important factor, along with vegetation, in producing better estimates

of evapotranspiration. This is possible due to the strong contrast between water and dry surfaces in the infrared (reflected) spectral region. Measurements of changes in the area of water bodies can be made using LANDSAT data (Barker, 1975) if there are sufficiently large variations.

Soil: The distribution of water and soil moisture is controlled by variations in soil types and precipitation. Fleming (1975) pointed out that soil may be classified from the hydrologic point of view by particle size, infiltration characteristics and profile type. This information is obtained from soil survey reports and laboratory tests.

Some studies have been carried out, however, to investigate if remote sensing can be used in mapping soil types and in detecting some soil characteristics at the regional level. It must be emphasized, however, that none of the available sensors is able to measure soil properties down the complete soil profile. The information that can be directly gathered is restricted to a thin layer of no more than 5 cm on top of the soil. (the part most affected by temporal changes). However, some soil characteristics can be inferred by analyzing soil spectral reflectance, colour, vegetation cover, land-use pattern, landscape and hydrologic behaviour. Under laboratory conditions, as well as from remote-sensing systems, it has been observed that particle size, texture, colour, organic matter and soil water content affect soil spectral response.

In general it can be concluded that LANDSAT data, either in

its photographic or digital format, has been successfully used in differentiating surface elements such as vegetation, water and soils. The repetitive coverage (18-day cycle), although not ideal when changes occur in shorter periods of time (eg. fires), allows the analysis of variations in spectral response of the elements as a product of seasonal and non-seasonal changes. The resolution of LANDSAT permits quantitative measurements using either visual or digital techniques.

2.4 Remote Sensing Applications to Hydrologic Models.

Some attempts have been made on an experimental and quasi-operational basis, to use remotely-sensed information as an input to hydrological mathematical models.

As already mentioned in Section 2.3.1, Follansbee (1973) improved Barrett's method for estimating 24 hour rainfall for large areas, using meteorological satellite imagery. The rainfall estimates were used as inputs to hydrologic models for simulating streamflow. Application of this method has been made in several tropical countries, basically for flood forecasting.

Amorocho (1975) used a similar approach based on ATS-3 geosynchronous satellite imagery for estimating 24 hr. rainfall, in the Sinú River of Colombia. The estimate of precipitation obtained for the upper portion of the basin and the data recorded in the lower part were used as input to a lumped conceptual model. The model was used to simulate discharge for engineering purposes (spillway design) and the results were highly satisfactory.

With regard to non-meteorological satellites, the first

attempt at using remote sensing as input was made by Ambaruch and Simmons (1974) using LANDSAT data. This study was developed from previous theoretical work carried out by them in 1973. The study was oriented to meet three main objectives:

- (1) To determine the optimal values and permissible tolerances of inputs to the model needed to achieve an acceptably accurate simulation of streamflow for the watershed,
- (2) To determine which model inputs can be qualified by remote sensing, directly, indirectly or by inference, and
- (3) To evaluate the required accuracy of remotely-sensed measurements to provide a basis for quantifying model inputs within permissible tolerances.

The model used in this experiment was the Stanford Watershed Model Version IV developed by Crawford and Linsley (1966). This is the best known and most widely used of all the deterministic lumped parametric models.

They arrived at the following conclusions:

- (1) At present remote sensing from space (LANDSAT) is applicable to the determination of model parameters related to physiographic characteristics, land use/land cover, snow coverage, water and impervious area.
- (2) At least eight parameters used in the model could be measured from LANDSAT data. With new improvements, basically in interpretation procedures rather than resolution, probably seven more new parameters can be added.

- (3) Permissible tolerances do not impose severe requirements on the resolution of the system (LANDSAT).

Ambaruch and Simmons (1974) suggested that to improve modelling by means of remote sensing, further study is required in the following aspects:

- (1) Soil surface and sub-surface characteristics,
- (2) Remote measurements of temporal phenomena such as precipitation, air temperature, relative humidity and evaporation rate,
- (3) Remote observation of snow pack depth at several points to estimate snow pack volume and water equivalent, and
- (4) Soil moisture measurements on daily basis within the watershed.

After Ambaruch and Simmons several studies have been carried out mainly dealing with the use of LANDSAT for extracting land use/land cover information for hydrologic models. Ragan and Jackson (1975, 1976) and Jackson et al. (1975) have used computer-compatible tapes to generate land use information required by a LANDSAT compatible version of the Soil Conservation Service (SCS) model. The results were considered as good as those obtained using high altitude aerial photography.

It can be noticed, however, that all the applications have been oriented towards mathematical lumped models, applied to urban basins of less than 5,000 km². It is suggested that the time is now right to investigate the application of satellite-generated data to deterministic distributed models, for large and ungauged watersheds.

CHAPTER 3

STUDY AREA AND DATA

3.1 Introduction

The objective of this chapter is first to describe the environmental characteristics of the selected study area. In the second part the platforms, remote sensing systems chosen and the data obtained are described. The third and last part is devoted to a discussion of the types of ground information used and the reasons for their selection.

3.2 Study Area

The area selected for this study is the Venezuelan Llanos¹. This distinct physiographic region covers approximately 28 % of the Orinoco River Basin (Figure 3.1). The Llanos are bounded by the Guayana Shield to the south and by the Andes and Coastal Ranges to the northwest and north respectively. The southwestern limit is the political boundary with Colombia, although the same physiographic unit continues into that country where it is known as the Llanos Orientales (Eastern Llanos).

Freile (1965) has stated that the Llanos in Venezuela can be divided into four physiographic sub-regions, namely:

¹ The term Llanos may be translated as grassy plains. It is a distinctive type of environment encountered in various parts of the world.

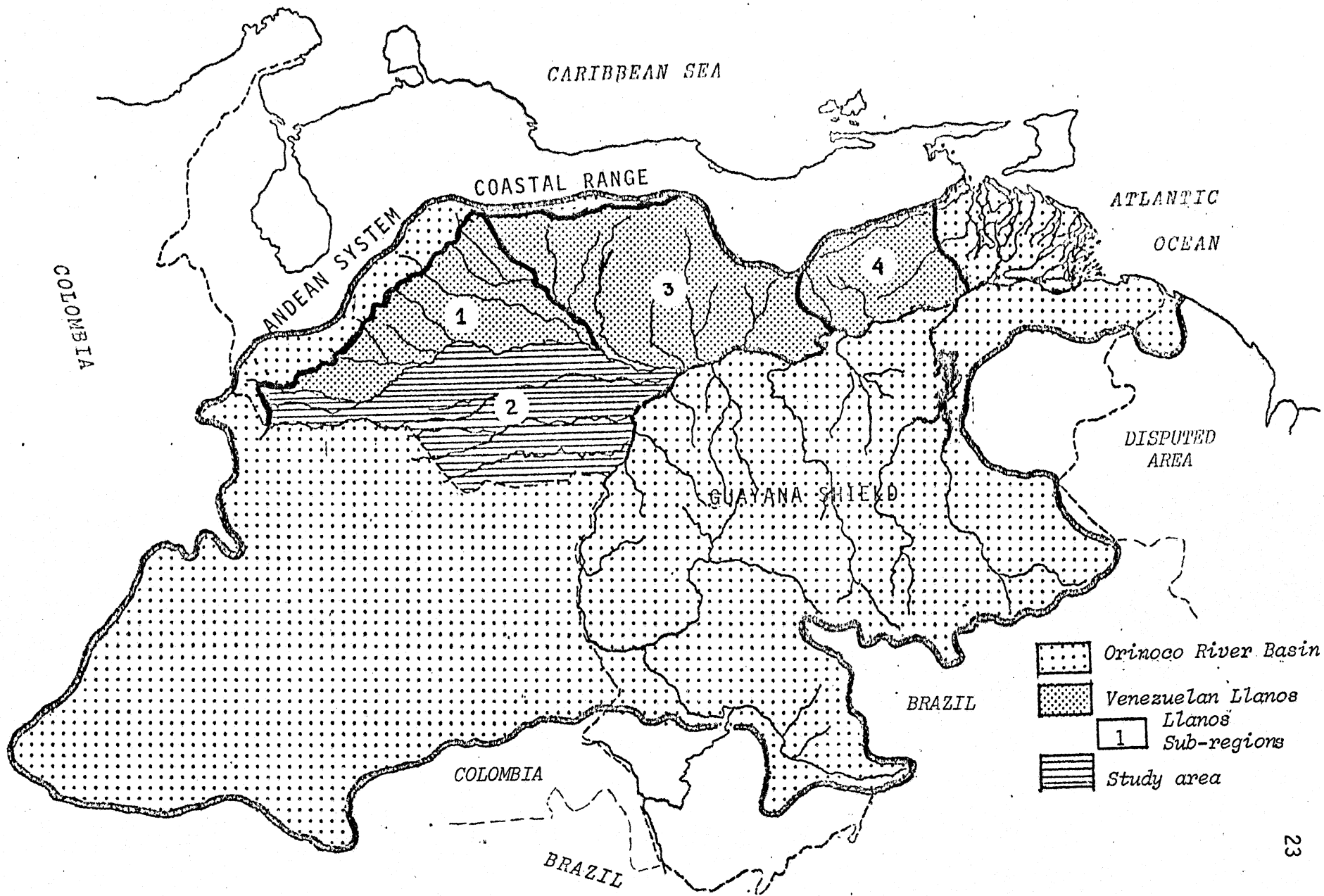


Figure 3.1 Location of the Venezuelan Llanos and Study Area.

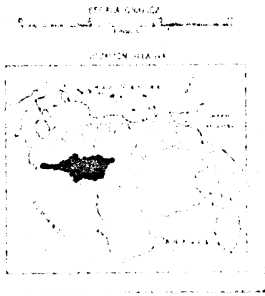
1. Llanos Occidentales of Barinas Portuguesa (Western Llanos)
2. Llanos de Apure (Apure Llanos)
3. Llanos Centrales o de Calabozo (Central Llanos)
4. Llanos Orientales o de Maturin (Eastern Llanos)

The work reported in this study is concentrated in the Apure Llanos sub-region. This area is characterized by a general low relief, although there are occasional areas of smooth and gently rolling hills, as well as isolated hills. The latter occur particularly along the western margins of the Orinoco River. The study area occupies the southern portion of the Apure sedimentary basin (Figure 3.2). The surface material consists primarily of unconsolidated Tertiary (Neogene) and Quaternary sediments, including recent alluvial deposits. The hills are composed of Precambrian rocks which are part of the Guayana Shield.

Using the terminology applied in a Biophysical Land Classification system (Lacate, 1969), three Land Districts¹ can be identified within the Llanos Land Region. These three Land Districts will be named Cinaruco High Plains, Capanaparo Sandy Plains and the Arauca-Apure Lowlands (Fig. 3.3). Their limits are almost equivalent to the High Plain, Aeolic Plain and Flood Plain areas designated by Comerma and Luque(1971).

To investigate the applicability of remotely-sensed information in hydrologic modelling, three river basins were selected, namely: the

¹ Land District is an area characterized by a distinctive pattern of relief, geology, geomorphology and associated regional vegetation.

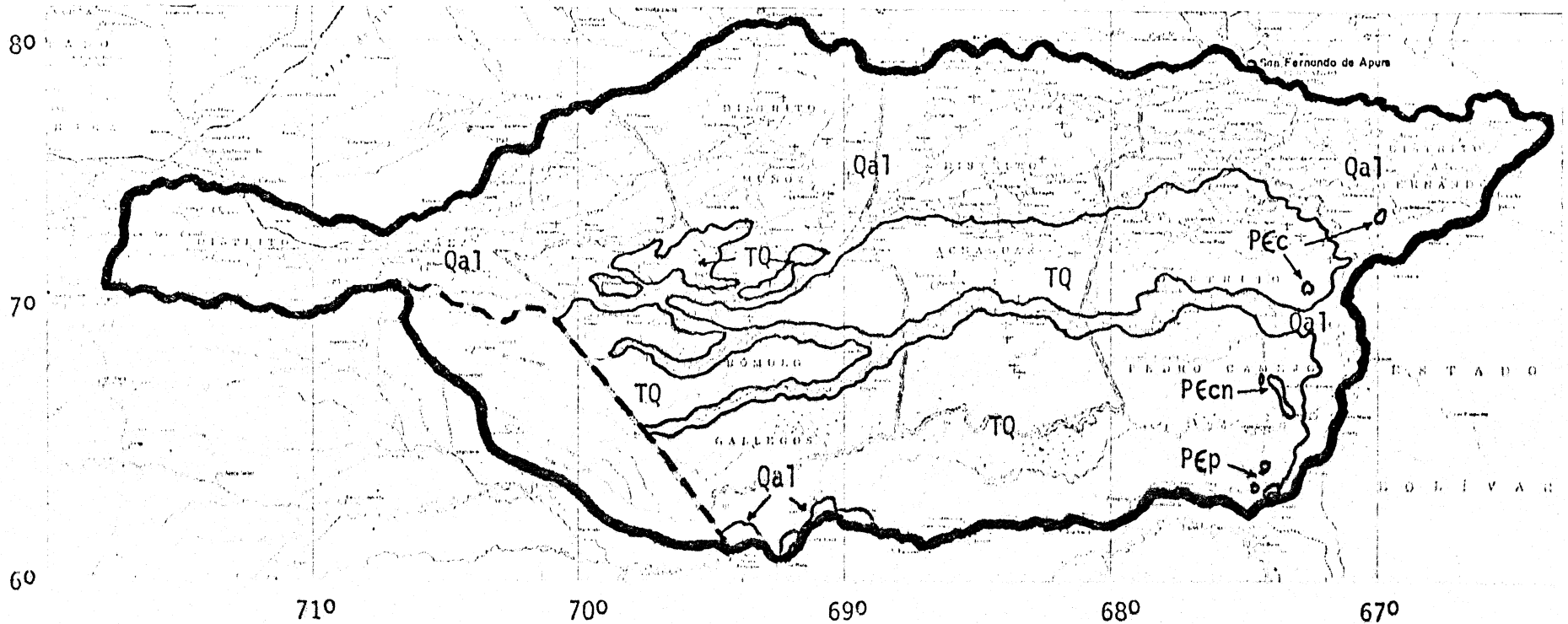


Qa1 = QUATERNARY (Alluvium)

P ϵ c, P ϵ p = PRE-CAMBRIAN (Plutonic rocks)

TQ = TERTIARY

P ϵ cn = PRE-CAMBRIAN (Gneiss, quartzite and schists)



Source: Ministerio de Minas e Hidrocarburos
(1972)

Figure 3.2 General Geologic Map of the Study Area.

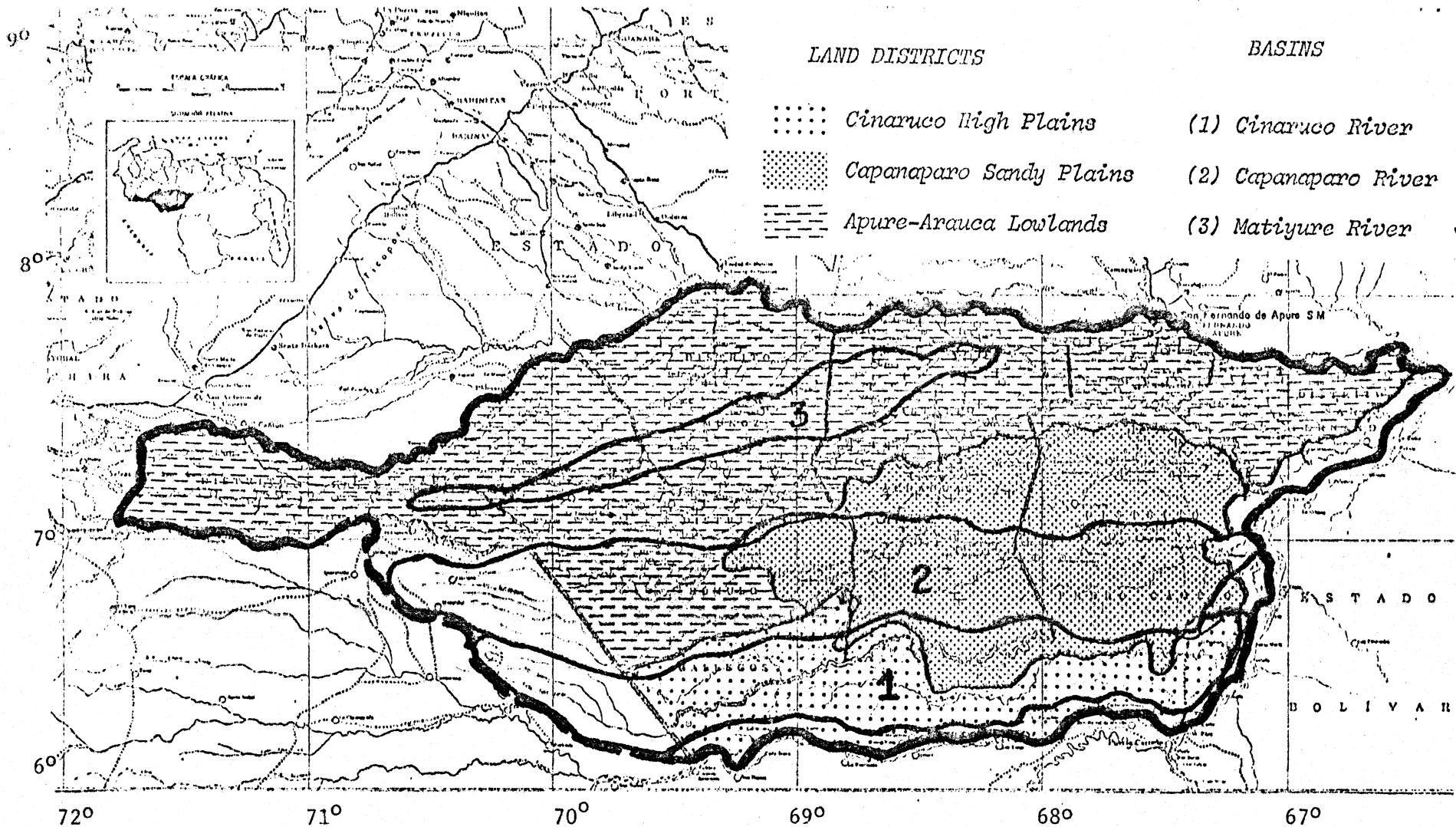


Figure 3.3 Apure Llanos: Land Districts and Basins Selected.

Cinaruco (9,900 km²), Capanaparo (19,450 km²) and Matiyure (6,530 km²) basins (Figures 3.4, 3.5, 3.6). There are several reasons for their selection:

- (1) The basins are representative of the different environmental and hydrologic conditions encountered in the Llanos. Each basin is located within a different Land District.
- (2) The availability of remote sensing data.
- (3) Hydrologic and meteorologic information are available for the period when the remote-sensing data were recorded.
- (4) The availability of background information on the geology, vegetation and soil characteristics of the area. This information can be used as an aid in the interpretation of the remote-sensing data.

Information on precipitation and temperature for the area, as well as other climatological parameters, is scarce. This problem is being solved, however, as the Venezuelan Government is now improving its network of meteorological stations. So far, rain gauges have been installed in several new locations (Figure 37) but information on temperature, radiation and evaporation are still lacking.

From the available data, it has been deduced that precipitation occurs in a very definite season from late April until late September. Some minor variations can be observed, depending on the location of the station. Precipitation increases towards the west and south (due to the effect of the Andes) and the south. Within the study area, maxima occur in the southern sector (Carabobo and Puerto Paez) and minima in the north-eastern sector (San Fernando and Corozo Pando), as shown in

Figure 3.4 Cinaruco River basin map.

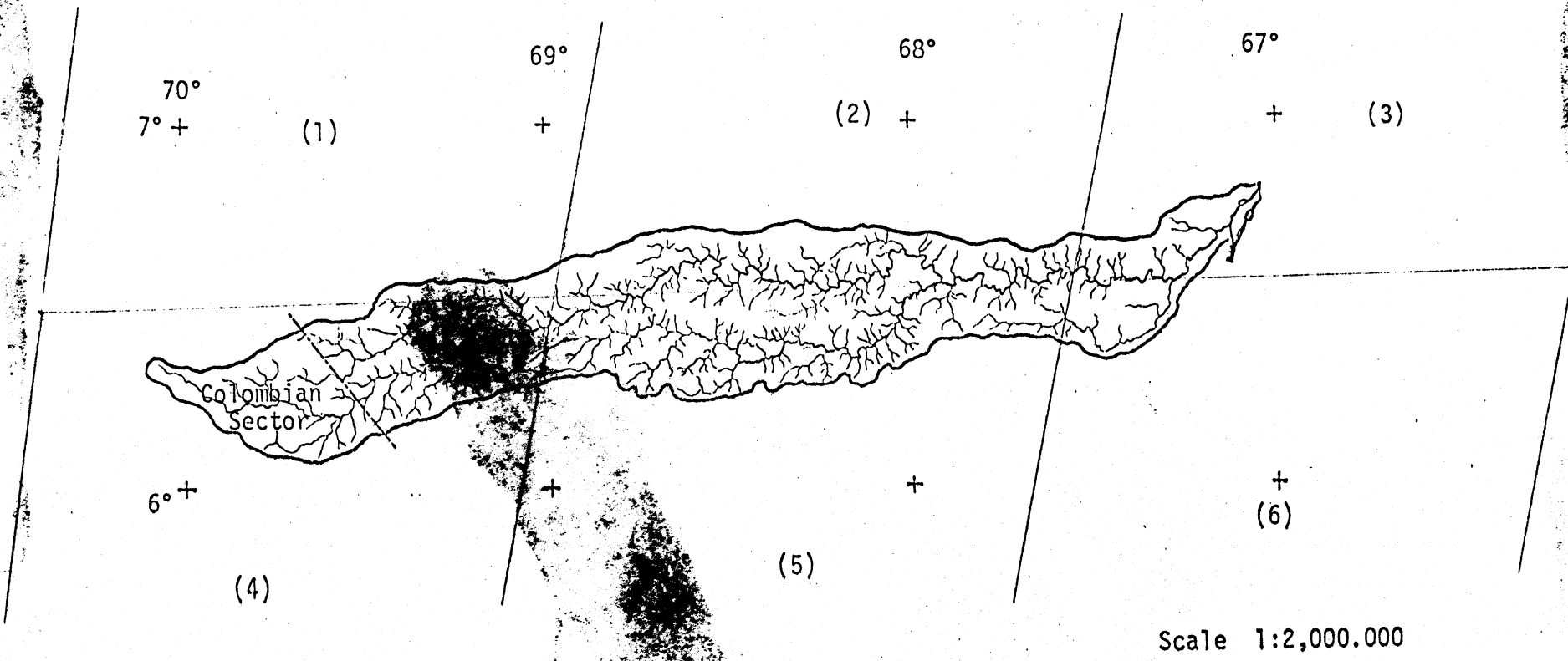


Figure 3.4 Cinaruco River basin map, produced from LANDSAT Images, (1) E-2029-14142, (2) E-1086-14194, (3) E-1229-14145, (4) E-1177-14255, (5) E-1194-14203, (6) E-1229-12151.

Figure 3.5 Capanaparo River basin map.

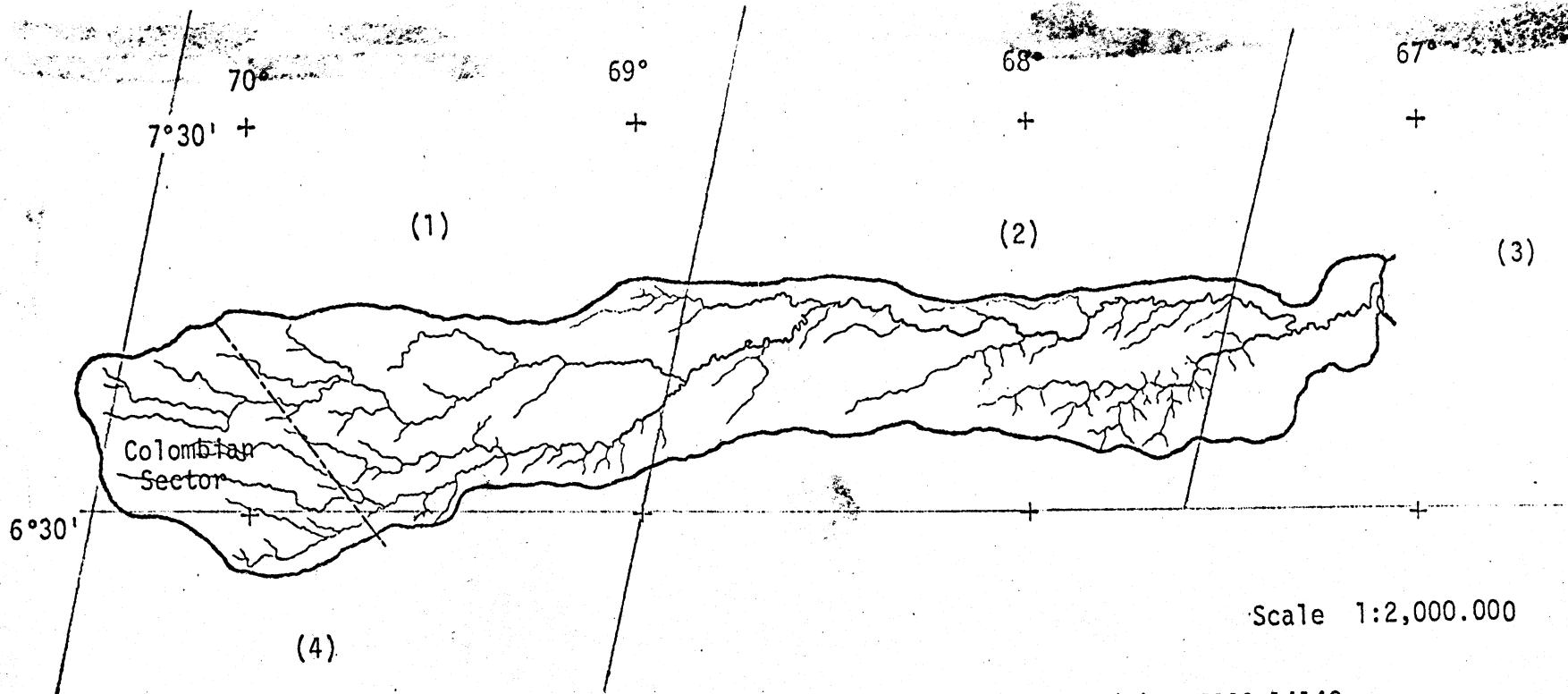


Figure 3.5 Capanaparo River basin map, produced from LANDSAT images, (1) E-2029-14142, (2) E-1086-14194, (3) E-1229-14145, (4) E-1177-14255.

Figure 3.6 Matiyure River basin map.

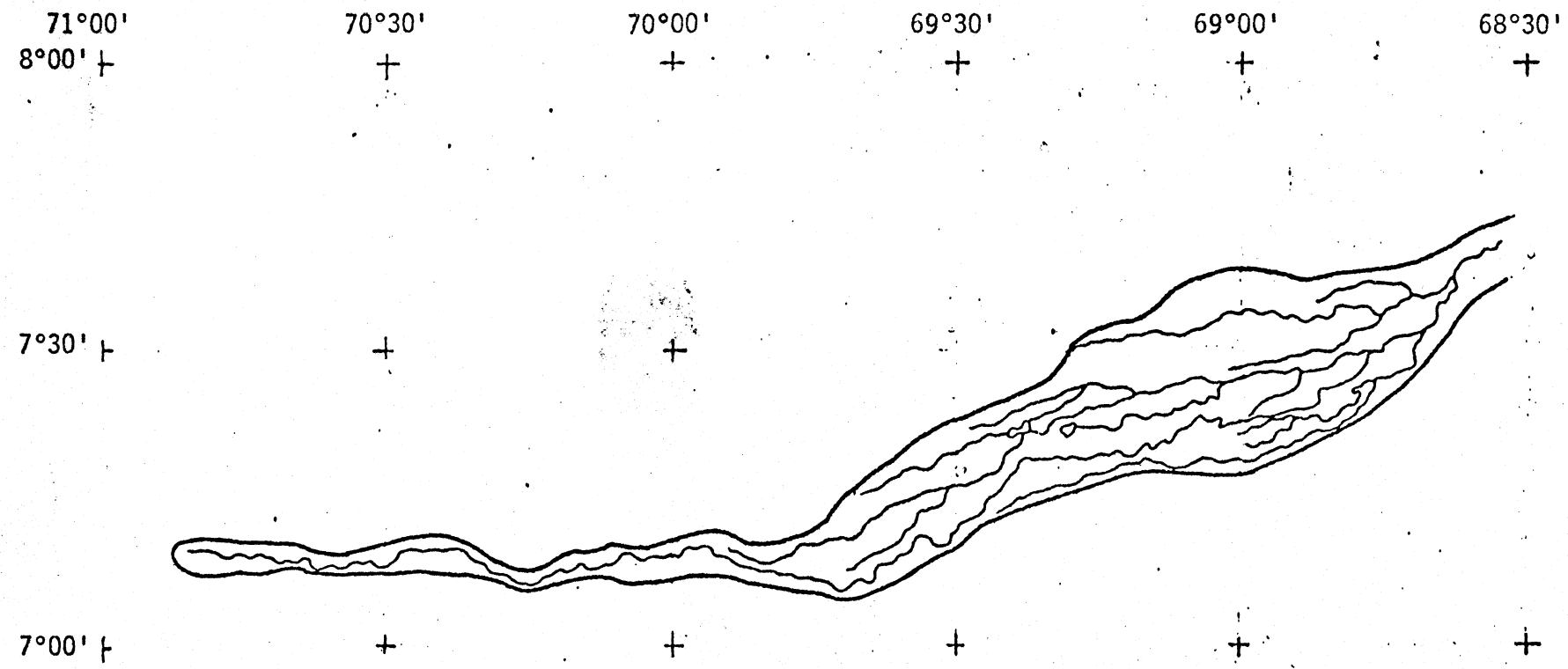


Figure 3.6 Matiyure River basin map, produced from LANDSAT image 2029-14142. Scale 1:1,300,000

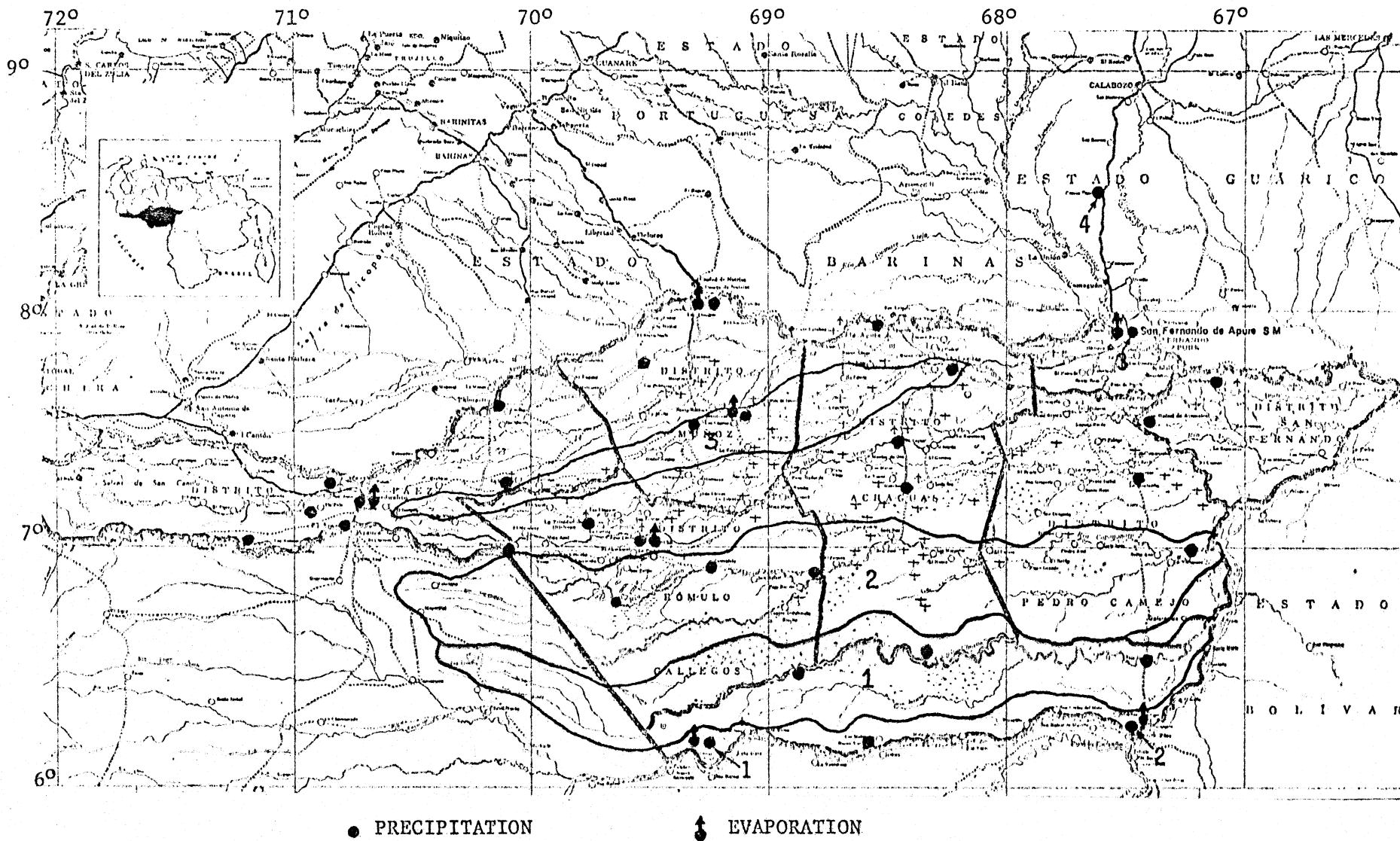


Figure 3.7 Location of meteorological stations.

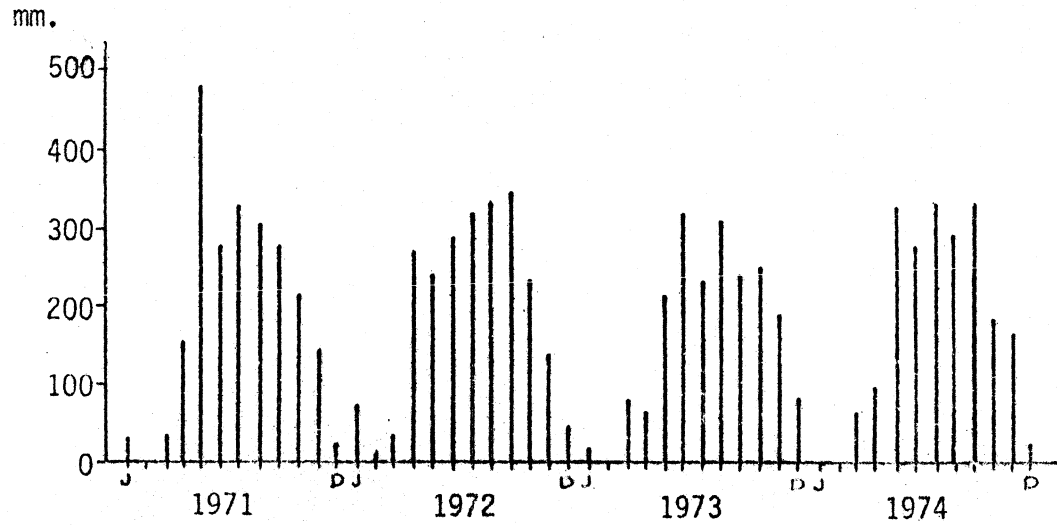
Figures 3.8 and 3.9.

Temperature data are available for only few stations, within the study area. From the analysis of the available data it can be concluded that temperature variations over the year are very small, averaging 2.5 °C. The daily variation is approximately 10°C.

With regard to soils, the information for the study area is also sparse. Some studies have been carried out at a reconnaissance level, by Desarrollo Industrial Agrícola C.A (DIACA C.A, 1958), Comerma and Luque (1971), Shargel and Gonzalez (1973) and Ministerio de Obras Publicas (1975). These soils studies are concentrated in the northern portion of the study area mainly around San Fernando de Apure and Bruzual-Mantecal sector. To meet the objectives of this research, the works done by DIACA C.A (1958) and Comerma and Luque(1971) were selected as the main sources of reference. There are two reasons for this. First, the soils are mapped at 1:500.000 which is a scale suitable for comparison with LANDSAT data. Other reports show more detailed information, but only for limited areas. Second, the vegetation and moisture conditions were used as elements in the classification.

Comerma and Luque (1971), identified four important landscapes within the Apure Llanos physiographic region. These are the Piedmont, the Flood Plain, the Aeolic Plain and the High Plains. The soil studies, however, were only carried out in the last three regions. The 7th approximation was the classification system used, and the results are presented in abbreviated form in Table 3.I and Figure 3.10.

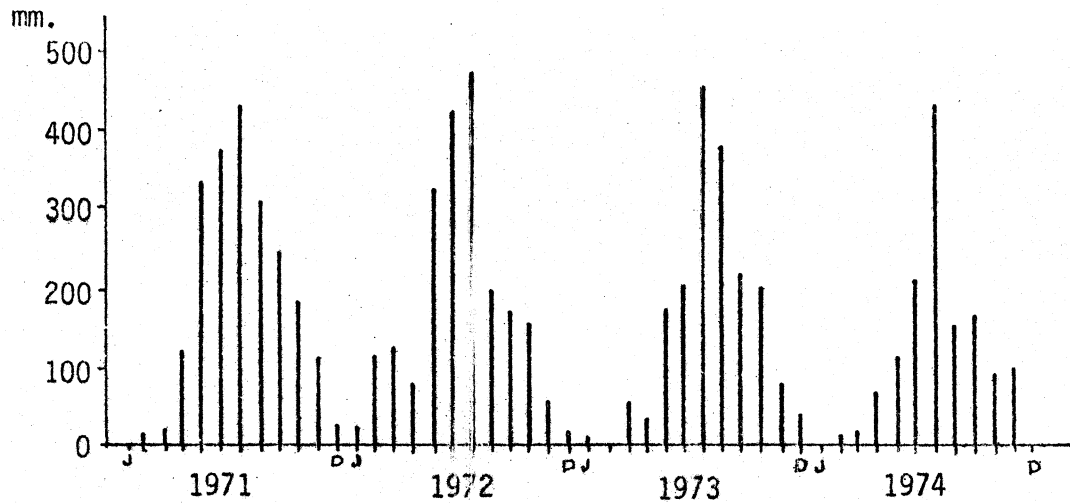
As far as vegetation is concerned, Sarmiento and Monasterio



STATION: CARARABO

LOCATION: 6°10'N , 69°16'W

NUMBER: 1 in Figure 3.7



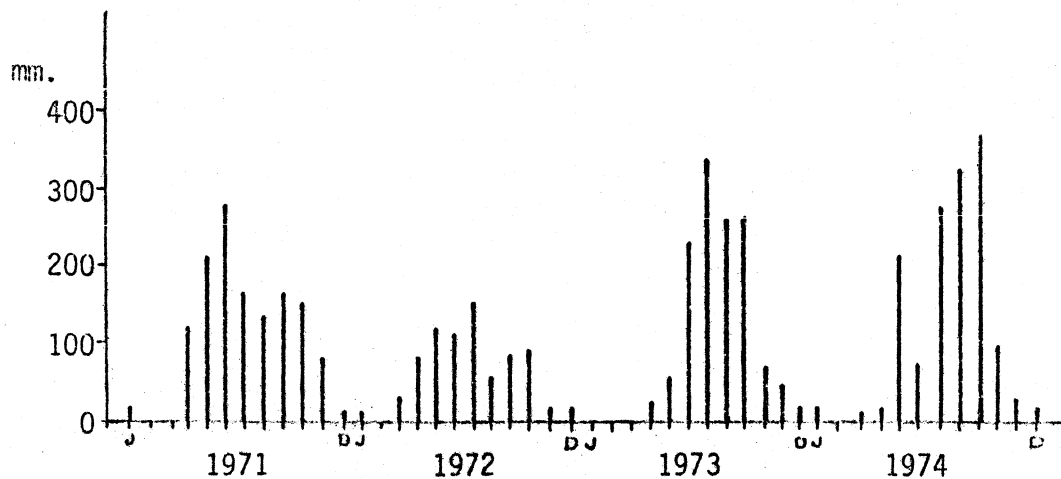
STATION: PUERTO PAEZ

LOCATION: 6°11'N, 67°27'W

NUMBER: 2 in Figure 3.7

Source: Ministerio de Obras
Públicas (1975)

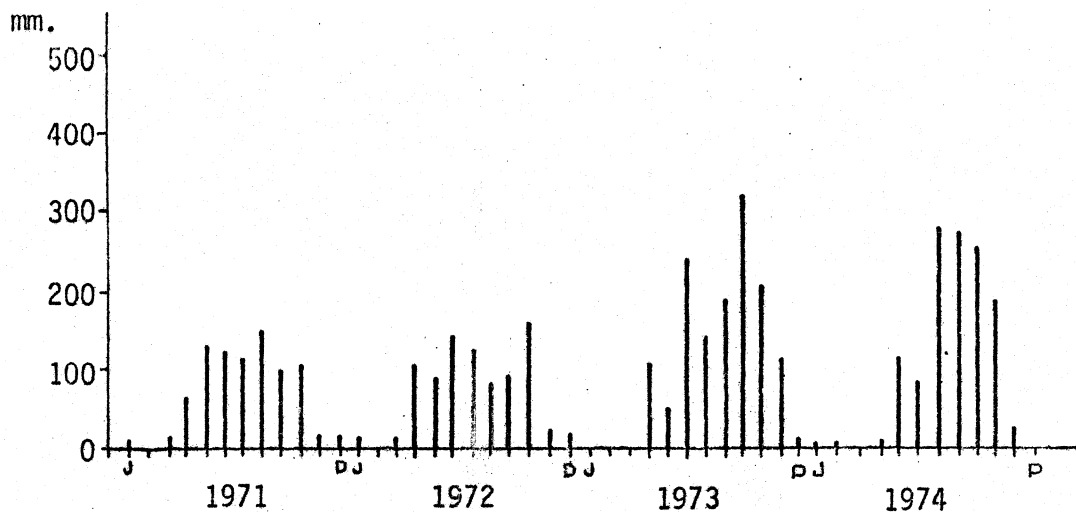
Figure 3.8 Monthly precipitation for Cararabo and Puerto Paez stations.



STATION: SAN FERNANDO

LOCATION: 7°54'N, 67°28' W

NUMBER: 3 in Figure 3.7



STATION: COROZO PANDO

LOCATION: 8°31'N, 67°33' W

NUMBER: 4 in Figure 3.7

Source: Ministerio de Obras
Públicas (1975)

Figure 3.9 Monthly precipitation for San Fernando and Corozo Pando stations.

TABLE 3.1

LANDSCAPES, SOIL TYPES, VEGETATION AND DRAINAGE CONDITIONS IN THE STUDY AREA

| LAND DISTRICTS | LAND SYSTEM ¹ | LAND TYPE ² | ORDER | SOILS | | VEGETATION | DRAINAGE CONDITIONS |
|----------------------|---|------------------------------|-------------------------|--|--|---|--|
| | | | | SUBORDER | DESCRIPTION | | |
| APURE-ARAUCA | Area with anastomosing drainage, gallery forest and subjected to flooding. | River banks | Inceptisols | Fluvents | Medium to fine texture, and acid soils. | Trees: <u>Samanea saman</u> (saman), <u>Guazuma ulmifolia</u> (guásimo). | Well to poorly drained soils. |
| | | "Bajfos" | Inceptisols | Aquepts | | Grasses: <u>Leersia hexandra</u> (lambedora), <u>Panicum elephantipes</u> (paja de agua). | Poorly drained soils. |
| | | "Esteros" | Vertisols | Usterts | | | |
| LOWLAND | Area with meandering rivers, without gallery forest and subjected to flooding | "Bajfos" | Inceptisols | Aquepts & Fluvents | Texture medium to fine, gray colour and yellow mottled. | Grasses: <u>Paspalum faciculatum</u> Willd (gamelote chiguirero). | Poorly drained (internally as well as externally). Areas with well drained soils only along the main rivers: Arauca and Apure. |
| | | "Esteros" | Entisols | Aquepts | | | |
| | Area subjected to occasional flooding. | River banks | Inceptisols Alfisols | Fluvents Ustalfs | Hidromorphic soils, with medium to fine texture and low organic matter content. | Grasses: <u>Axonopus sp</u> | Poorly drained soils. During the rainy season this area is covered by a shallow layer of water which is lost by evaporation. |
| "Bajfos" | Inceptisols | Aquepts | | | | | |
| "Esteros" | Vertisols | Uderts and Usterts | | | | | |
| CAPANAPARO | SANDY PLAINS | Sand dunes | Entisols | Psamments | Soils formed by 93% sand and 2-5% of clays. Organic matter only is 10 to 15 cm depth. | Trees: <u>Byrsonima</u> and <u>Curatella</u> (chaparro), <u>Bowditchia virgiloides</u> , H.B.K. (alcornoque). Grasses: <u>Trachypogon sp</u> (paja saeta), <u>Paratheria prostrata</u> (paja carretera). | Very well drained soils. |
| | | Sand field and flat surfaces | Ultisols | Ustolts | Sandy soils with deeper organic matter layer (15 cm). Plinthite at 50 to 100 cm depth. | Trees: <u>Mauritia minor</u> , Burret (palma moriche) along the river channels. <u>Paratheris prostrata</u> (paja carretera). | Well to poorly drained soils. |
| CINARUCO HIGH PLAINS | Smooth rolling hills | Ultisols | Ustolts | Medium texture, red, and lower organic matter content soils. (pH 5.0). | | | |
| | | Oxisols | Ustoxs | | | | |
| | Flat surfaces | Ultisols | Aquults | Medium texture with slope less than 0.5%. | Grasses: <u>Trachypogon sp</u> (paja saeta), <u>Paspalum plicatum</u> , <u>Michx</u> (gamelotillo) | Medium to poorly drained soils. | |

1. Land system is an area of land with a recurring pattern of land forms, soils and vegetation. (Lacate, 1969).

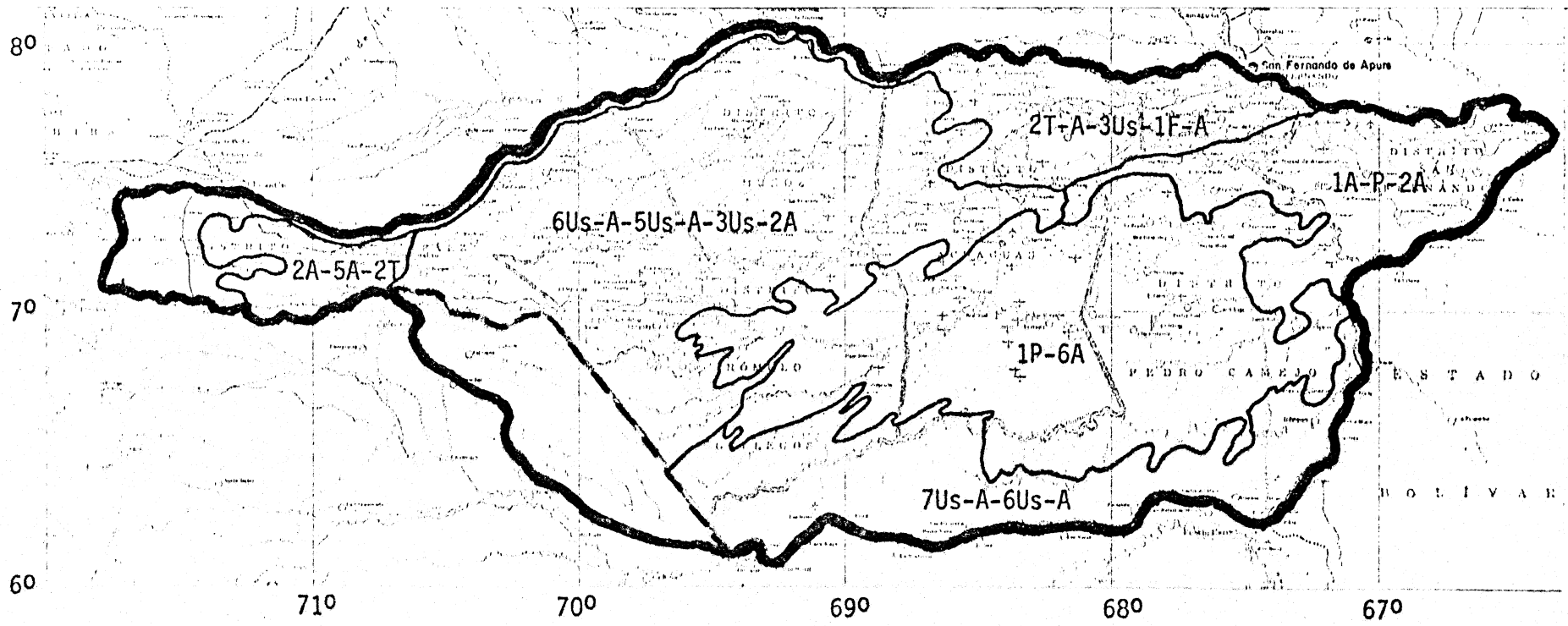
2. Land type is a land area with a characteristic parental material with a fairly homogeneous soil and vegetation chronosequence. (Lacate, 1969).

Based on: Comerma and Luque, (1971).



SOIL ORDERS AND SUBORDERS (7th Approximation)

- | | | | | | |
|----------------|---------------------------------------|--------------|-------------------------|-------------|-------------------------|
| 1. ENTISOLS | A=Aquents F=Fluents P=Psamments | 3. VERTISOLS | Us=Usterts | 6. ULTISOLS | A=Aquults Us=Ustults |
| 2. INCEPTISOLS | A=Aquepts T=Tropepts | 5. ALFISOLS | A=Aqualfs Us=Ustalfs | 7. OXISOLS | A=Aquoxs Us=Ustoxs |



Source: Ministerio de Agricultura y Cria (1974)

Figure 3.10 General soil map of the study area.

(1969) found four different areas within the Venezuelan Llanos. These areas were designated as:

- (1) Tropical Deciduous Seasonal Forest,
- (2) Semi-evergreen Forest,
- (3) Wet Savanna, and
- (4) Dry Savanna.

The approximate extent of each of these areas is shown in Figure 3.11 .

Detailed studies of the vegetation communities in the study area do not exist. Analysis of the distribution of the dominant vegetation communities (savannas and forests) however, has been carried out as supplementary information for the soil and geomorphological studies by DIACA C.A (1958) and Comerma and Luque (1971).

The present study area corresponds to the so called dry savanna of Sarmiento and Monasterio (1969). Significant variations in vegetation communities occur, however, within this region. The variations are a result of different soil types and moisture conditions encountered in the region.

3.3 Remote-Sensing Data.

The remotely-sensed data used in this research were obtained from both the SMS-GOES and the LANDSAT satellites.

The SMS-GOES satellites are placed in a circular, geostationary or geosynchronous orbit over a fixed point on the earth's equator. This type of orbit allows the system on board the satellite to record data on a continuous basis.

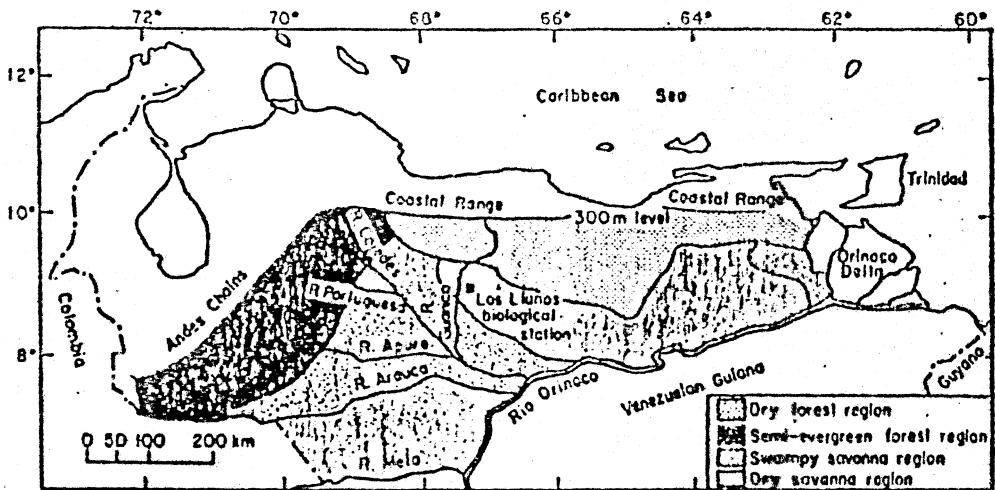


Figure 3.11 Venezuelan Llanos: vegetation regions.

Source: Sarmiento and Monasterios (1969)
(p. 581)

Two sensor systems are on board the SMS-GOES satellites. These are the visible and Infrared Spin-scan Radiometer (VISSR) and the Space Environmental Monitor (SEM). The latter is used to provide measurements of sun activity and thus will not be considered in this research.

The VISSR sensor records data from the earth's surface from west to east in eight visible and two infrared spectral channels. A complete image of the earth's disc is reconstructed from north to south every 18.2 minutes. The maximum resolution is 0.7 km for the visible bands (.55 to .70 μm) and 8.0 km for the infrared images (10.5 to 12.6 μm).

The SMS-GOES satellites are able to relay information from Data Collecting Platforms (DCP's). The system is capable of handling a maximum of 10,000 DCP's.

The imagery used in this research was obtained from the National Oceanographic and Atmospheric Administration (NOAA) of the United States and from the Ontario Centre for Remote Sensing, Canada.

Two Earth Resources Technology Satellites (LANDSAT-1 and LANDSAT-2) have been in operation since 1972. They were placed in a sunsynchronous orbit allowing the observation of the same point on the earth's surface every 18 days, approximately at the same local time.

Three sensor systems are mounted in the spacecraft, the Multispectral Scanner (MSS), the Return Beam Vidicon (RBV) and the Data Collecting System (DCS). The MSS and the RBV systems generate images of the earth's surface beneath the spacecraft. The DCS relays information (eg. temperature, stream levels and wind velocity) from remote Data Collection Platforms (DCP's). The two latter systems were not used in this project and thus will not be considered in it.

The Multispectral Scanner Systems (MSS) oscillating mirror continuously searches information in a strip 185 km wide from directly beneath the satellite. The reflected energy is recorded simultaneously by six detectors grouped in four spectral bands from 0.5 μm to 1.1 μm .

The instantaneous field of view (IFOV) for each detector is a rectangular area at the earth's surface measuring 79 m on a side. Every 9.95 μsec the rectangular surface is sampled in the crosstrack direction, corresponding to an equivalent ground motion of 56 m.

Each rectangle of approximately 79 x 56 m is called a picture element or pixel. Approximately 3,200 of them are generated in each sweep. The data is recorded continuously. As each image contains around 2,400 lines, more than 7.5×10^6 pixels are thus generated for each spectral band.

The reflected energy is focused onto a detector which measures the amount of energy for each pixel. In each band and for each pixel the reflected energy is recorded as a numerical value from 0 to 63. The value 63 is equivalent to the highest amount of energy and 0 to the lowest. For each pixel four different values are recorded corresponding to each of the four spectral bands. Normally the set of four values is called the spectral signature or intensity vector for the pixel (Howarth, 1976).

The data can be either recorded or transmitted in real time. In the Venezuelan case, the data are recorded and stored on the wide-band tape recorder carried on the satellite. Later on the data are transmitted to any of the receiving stations (U.S.A or Brazil), when the satellite is within reception range. The data may be analyzed in

its digital format or may be transformed into imagery covering 185 x 185 km.

The LANDSAT imagery and computer compatible tapes were available as a result of a cooperative programme established in April, 1972 between the former Ministerio de Obras Públicas (now Ministerio de los Recursos Naturales y del Ambiente), Dirección de Cartografía Nacional, Venezuela, and the National Aeronautics and Space Administration (NASA) of the United States.

The imagery was processed and supplied by the Departamento de Sensores Remotos, Dirección de Cartografía Nacional (Venezuela). Colour composites and computer compatible tapes were obtained from the EROS Data Center, of the United States Geological Survey.

3.4 Ground Data

Ground information for the present study was obtained from the publications by Desarrollo Industrial Agrícola C.A (DIACA), 1958 and Comerma and Luque (1971). The purpose of their studies was to provide information about the major landforms, soil types and vegetation present on the Llanos de Apure. The information contained on the maps and in the report was considered suitable for this research. This information was selected, due to the impossibility of carrying out detailed field work for this report.

CHAPTER 4

APPLICATIONS OF GOES-1 DATA TO HYDROLOGIC DISTRIBUTED MODELS

4.1 Introduction.

This chapter considers the meteorologic satellite data (GOES-1) as a source of distributed information on precipitation that can be applied in hydrologic models. The evaluation was carried out to meet two objectives:

- (1) To test the value of meteorological satellite data in analyzing the temporal and areal distribution of precipitation,
- (2) To select an adequate method for estimating precipitation from satellite data.

4.2 Analysis of GOES-1 Data.

The material used in this research consisted of weather facsimiles (WEFAX) and photographic copies from GOES-1 satellite. The WEFAX originals were reproduced from the archives of the Ontario Centre for Remote Sensing using a 35 mm camera loaded with high contrast film. During the reproduction process care was taken to maintain the same illumination thereby avoiding data distortion.

The GOES-1 data is available in two spectral bands, one visible and one thermal infrared (Table 4.I). Temperature enhancement of the infrared data is carried out to aid the identification of significant

TABLE 4.1

FORMAT OF GOES-1 (75°W 0°)

| <i>Nº</i> | <i>Format</i> | <i>Spectral Band</i> | <i>Resolution</i> | <i>Availability</i> |
|-----------|-------------------|----------------------|-------------------|---------------------|
| 1 | Full Disc WC-1 | Visible | 3.7 km | At CDDF and EDS |
| 2 | UC-1 | Visible | 3.7 km | Transmitted (WEFAX) |
| 3 | WB-1 | Visible | 1.9 km | At CDDF and EDS |
| 4 | Full Disc IR | Infrared | 9.3 km | Transmitted (WEFAX) |
| 5 | UC-1 IR | Infrared | 9.3 km | Transmitted (WEFAX) |

After: Corbell et al. (1976)

clouds and surface features (Figures 4.1 and 4.2). Further information about these techniques and about the GOES system can be obtained from Corbell et al. (1976).

4.2.1 Analysis of the Temporal and Areal Distribution of Precipitation based on Goes-1 Data.

Analysis was carried out using data from the WEFAX system. Due to resolution limitation of this system the analysis had to be carried out over the Apure Llanos as a whole. Using hard photographic copies or digital data it should be possible to obtain higher resolution for the study of smaller areas.

The imagery used in this research was recorded between June 1st and July 15th 1977, before the maximum activity of the Intertropical Convergence Zone (ITCZ) occurred over the study area.

The ITCZ¹ has been identified as the most important factor controlling weather over tropical areas, its effects being primarily reflected in rainfall activity. On an individual satellite image, the ITCZ exhibits a complicated structure comprising several cloud clusters separated by clear skies (Holton et al., 1971).

With regard to the study area, the passage of the ITCZ produces a noticeable increase in precipitation as seen in Figure 3.8 and 3.9. This occurs from April to November with a maximum around July. The months of April, July and November correspond to the advance, maximum activity.

¹ The ITCZ is a narrow east-west band of heavy cumulonimbus convection resulting from the contact of the two trade winds. It produces heavy precipitation.

1500 24AU76 23A-2 00101 19111 WC1

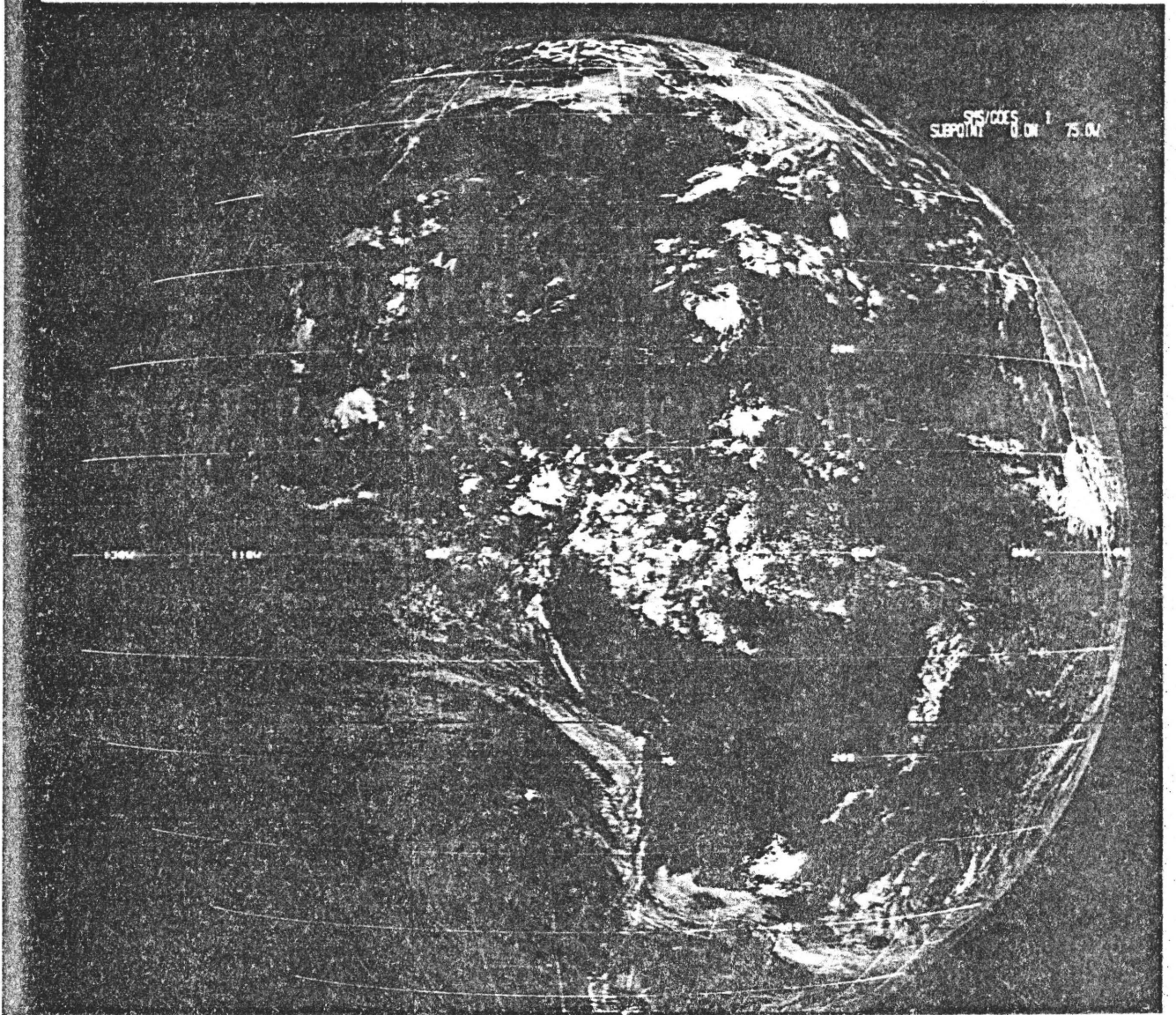


Figure 4.1 GOES-1 image of the visible spectral band (WC-1)

↑ 14:00 24AU76 13A-Z 0006-1640 FULL DISC IR

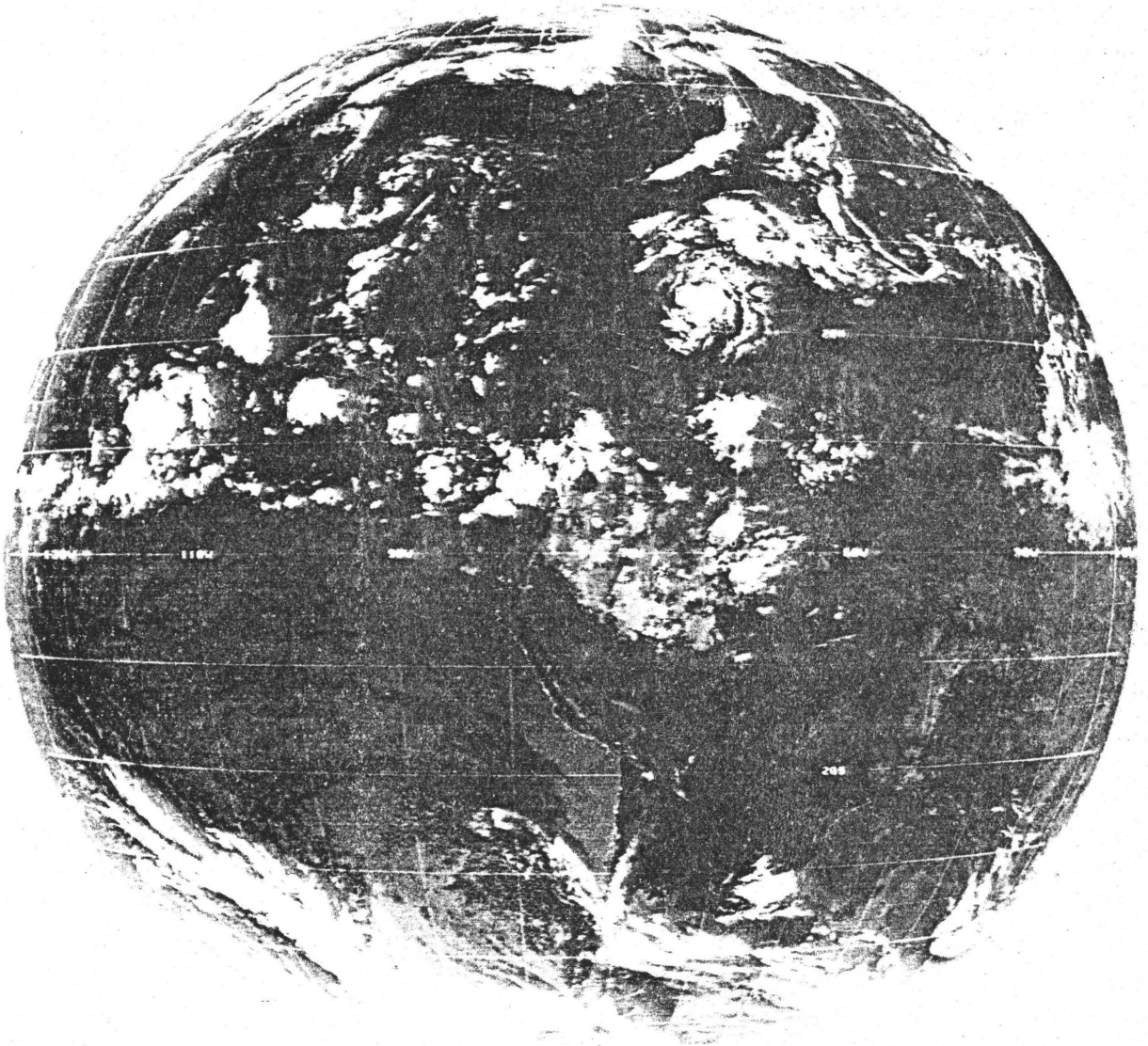


Figure 4.2 GOES-1 image of the thermal infrared spectral band.

and retreat of the ITCZ respectively. The location and degree of intensity of the ITCZ can be observed using the Full Disc (Visible or IR) imagery as shown in Figures 4. 1 and 4. 2

GOES-1 sensors generate images every 30 minutes, as is shown in the sequence recorded on June 10th 1977 (Table 4. II and Fig. 4.3). This coverage allows the continuous monitoring of cloud activity on a given area. The size of the area, as well as the cloud or clouds clusters that can be detected, will depend on the resolution of the data used. The maximum resolution of GOES-1 data is 1.9 km (WB-1 Sector) in the visible band and 9.3 km (UC-1, IR) for the thermal region in the type of data used for the study area.

Rain-producing clouds such as cumulonimbus, cumulus congestus and nimbostratus are generally well developed in size and cover relatively large areas, particularly in tropical areas. Therefore, their detection is not difficult using high resolution satellite imagery.

4.2.2 Precipitation Estimates Using GOES-1 Data.

The areal variability of precipitation is a major problem when estimating average rainfall over large areas. The methods available (Arithmetic Mean, Thiessen Polygons and Isohyetal) are highly dependent on rain gauge distribution. None of the above techniques can be relied upon when dealing with large and poorly instrumented basins, as is the case of the study areas (Figure 3.7).

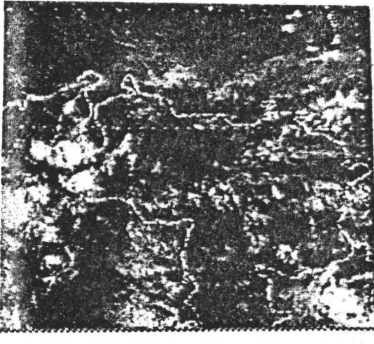
However, the extensive coverage and the resolution of GOES-1 data allows the location of cloud types. This allows the identification of areas where precipitation is most likely to occur. Catalogues for

TABLE 4.II

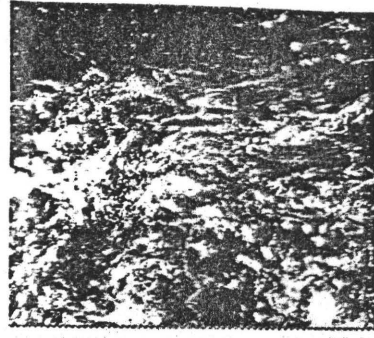
GOES-1 IMAGERY RECORDED
ON JUNE 10, 1977

| <i>Date</i> | <i>Format</i> | <i>Time</i> | |
|---------------|---------------|-------------|--------------|
| | | <i>GMT</i> | <i>Local</i> |
| June 10, 1977 | DC27N90W-1 | 10:30 | 06:30 a.m |
| | DC27N69W-1 | 12:30 | 08:30 a.m |
| | DC27N69W-1 | 13:00 | 09:00 a.m |
| | DC27N69W-1 | 16:30 | 12:30 p.m |
| | Full Disc IR | 17:00 | 01:00 p.m |
| | DC27N69W-1 | 18:00 | 02:00 p.m |
| | DC27N69W-1 | 19:00 | 03:00 p.m |
| | DC27N69W-1 | 19:30 | 03:30 p.m |
| | DC27N69W-1 | 20:01 | 04:01 p.m |

Source: Ontario Centre of Remote Sensing (GOES-1 Archives)



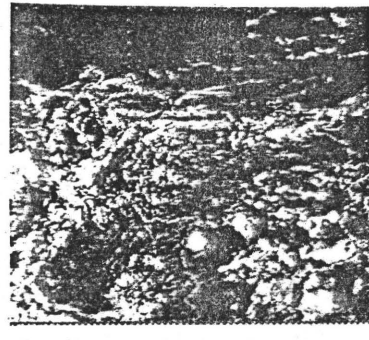
12:30 GMT



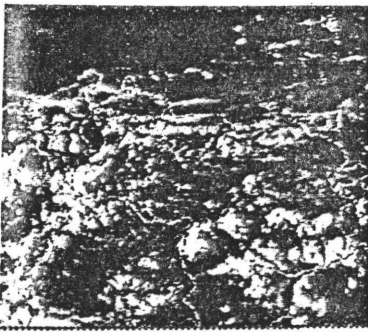
16:30 GMT



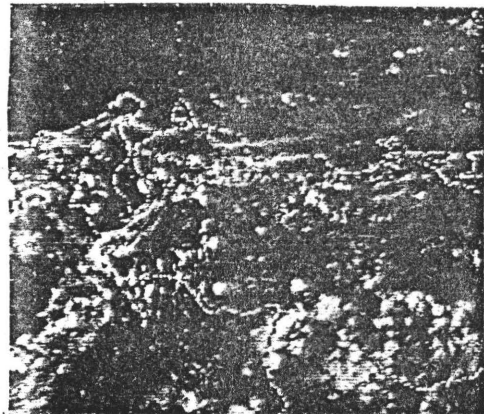
17:00 GMT



18:00 GMT



19:00 GMT



20:01 GMT

Figure 4.3 GOES-1 image sequence taken on June 10, 1977.

for identifying the different types of clouds have been published (e.g Conover, 1962).

Several methods have been developed to estimate precipitation using meteorological satellite data. Follansbe (1973) developed a method based on Barrett's approach for estimating 24 hr. rainfall from satellite imagery. The method, although empirical, has been found useful and its application has produced satisfactory results in several areas of the world, notably in the United States (Central and South) and Zambia.

The 24 hr rainfall estimate of the area is based on cloud identification from the satellite imagery. The following equation is then applied:

$$R_e = \frac{K_1 C_1 + K_2 C_2 + K_3 C_3}{100}$$

where:

R_e = 24-hr variable estimate for the area, in inches

C_1 , C_2 , and C_3 = are the percentages of the area covered by the rain-producing clouds: cumulonimbus, nimbostratus and cumulus congestus.

K_1 , K_2 , and K_3 = are empirical coefficients for each of the different cloud types.

Several applications of the method have shown that optimum values for the coefficients are: $K_1 = 1.0$, $K_2 = 0.25$ and $K_3 = 0.02$.

Therefore the final equation is:

$$R_e = \frac{1.0 C_1 + 0.25 C_2 + 0.02 C_3}{100}$$

The coefficients are calculated using the formula:

$$K = \frac{R}{C}$$

where: R = is the average of the rain collected by all gauges in the area on a given day in hundredths of an inch.

C = is the percentage of cloud cover at the time the image is recorded.

This methods assumes that the image selected (preferably one in the afternoon) is representative of the day. Also it can be observed that the maximum estimate of precipitation that can be obtained by this method is 25,4 mm (1 inch) for a 24-hr period if the selected image of the area under study displays 100 % cumulonimbus cover.

Using the continuous coverage of GOES-1, the risk of selecting an inappropriate representative image can be avoided. Furthermore, it has been found that in tropical areas large amounts of precipitation can fall late in the evening or at night. Thus estimates are unlikely to be very accurate. The cloud activiy at night can be monitored using the thermal infrared imagery, although the identification of small individual clouds is limited by the resolution of 9.3 km.

It has also been found that in tropical areas, particularly those affected by the ITCZ, estimates of precipitation from satellite data are lower than observed. Follansbe tested the method in the Suriname river basin of Surinam (East of Venezuela) and found that the coefficient for cumulonimbus (1.0) must be multiplied by 3 to produce better estimates during the rainy season.

To be able to apply this method to hydrologic distributed models, some modifications are required. These will be discussed in the next section.

4.3 Discussion.

The method developed by Follansbe is to obtain estimates of precipitation on a 24-hr period basis. This time interval, however, is not suited to most hydrologic models.

As previously mentioned, GOES-1 sensors generate data every 30 minutes. It is suggested therefore that the approach can be adapted to estimate precipitation values over large areas for time intervals of less than 24 hr.

The time interval most frequently used in hydrologic models is 1 hr. For this time interval the values of K are obtained using the average rain (R) of all the stations in the area for the 1 hr-period and the percentage of each type of cloud cover on the image taken at the time of precipitation measurement.

The use of GOES-1 data is limited by its resolution. For distributed models, the minimum area over which rainfall estimates can be obtained using the WB-1 Visible Sector format is of the order of $1.9 \times 1.9 \text{ km}$ (3.61 km^2).

The selection of the size of the unit element must be based on the following factors:

- (1) The resolution of the satellite data, as already mentioned,
- (2) The size of the area to be studied,
- (3) The amount of information required.

The time interval over which the calculations are carried out for each one of the unit elements is determined by:

- (1) Time interval of data acquisition by the satellite,
- (2) Time interval of the hydrologic model.

When the size of the unit element and the time interval have been selected the process is quite straightforward, and the steps to follow are:

- (1) Identification of the unit element in which cloud or cloud clusters occurs (Fig. 4.4)
- (2) Recognition of the different type of clouds. Estimate percentage of cover of each one of the types
- (3) At unit element level the weighted coefficient is calculated and applied to estimate precipitation.

Uneven distribution of rain gauges, discontinuous information and delay in data distribution are problems that have to be solved when studying large drainage basins. It can be concluded that GOES-1 satellite data can be used to partially overcome these problems because of its continuous coverage, spatial resolution and near-real time mode of operation.



Figure 4.4 GOES-1 image of the visible band showing the grid elements

CHAPTER 5

EVALUATION OF LANDSAT DATA

5.1 Introduction.

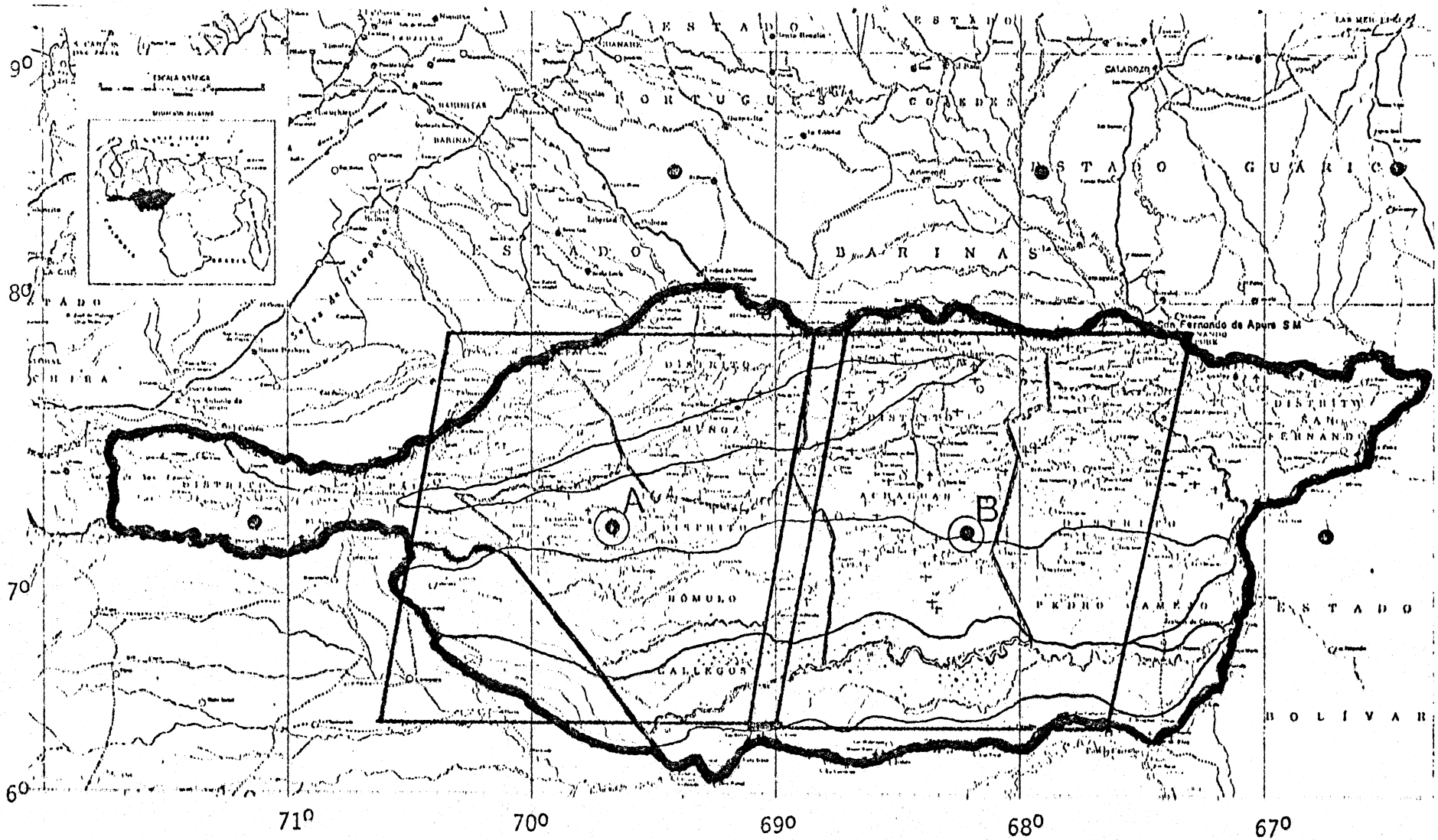
The objective of this chapter is to demonstrate the possibilities of LANDSAT data, as a source of information in determining land use/land cover and soil characteristics for hydrologic distributed models. The data used was composed by black and white transparencies of Band 5 and 7 and colour composites made from Bands 4,5 and 7. Also computer compatible tapes (CCT's) were used in the evaluation.

Several LANDSAT images are required to cover the study area, as shown in Figure 5.1. Because of this, a selection of representative imagery was required. Two images were selected and they are identified as A and B in Figure 5.1. In the selection of the images care was taken to include all the environmental conditions of the study area.

From the computer list, imagery was also selected to represent the DRY and WET or RAINY seasons. This selection is of particular interest for the analysis of seasonal variations in vegetation cover, surface water and surface soil moisture.

Only one CCT was available for this project and that was the image E-2029-14142 recorded on February 20, 1975 by LANDSAT-2. Part of the Matiyure River basin is covered by this tape.

The information was extracted from the appropriate data sources using visual, optico-mechanical and digital techniques. Instruments



● Imagery available (center) ⊙ Imagery selected

Figure 5.1 LANDSAT coverage of the study area.

located at McMaster University, the Ontario Centre for Remote Sensing and the Canada Centre for Remote Sensing, were used in this project.

5.2 Visual Analysis.

5.2.1 Introduction.

Visual analysis was carried out using imagery of the three basins, namely Cinaruco, Capanaparo and Matiyure. However in this section only the results obtained in the Cinaruco and Capanaparo basins will be discussed. The results for the Matiyure basin will be considered in the section on digital analysis.

To generate the photographic products the reflectance values in each band recorded for all the pixels in the range 0-63 are used to generate 15 gray tones, including black and white. This process is performed by an Electron Beam Recorder. The final product is a set of transparencies of approximately 1:3,3 million scale on 70 mm film. From these, enlargements to 1:1,000,000 are prepared as a basic output of the system.

When the information is translated from the digital form into the photographic form, a degradation of data occurs. Alföldi (1975) pointed out three reasons for this: (1) The consistency in the photographic process is difficult to maintain. (2) The radiometric range and resolution is lowered in the photographic product. (3) The spatial resolution is also degraded. It has been found, however, that a great deal of information can be extracted by visual analysis of the photographic product. Alföldi (1975) holds that the advantages of the

Photographic products are: (1) Less expensive than digital tapes, (2) Easy to handle and store, (3) Less vulnerable to damage, (4) The format is familiar to greater number of people, (5) The information contained in an image is easily extracted without any sophisticated instruments and (6) The machinery to enhance the photographic data is more economical and less difficult to operate.

Colour composites and black and white 1:1,000,000 transparencies were selected for the visual analysis. The selection of this material was based on the fact that the photographic transparencies has better definition than photographic paper.

The visual analysis of LANDSAT images of the Cinaruco and Capanaparo river basins was carried out in two stages:

- (1) Analysis of single data image,
- (2) Analysis of multivariate imagery.

5.2.2 Visual Analysis of Single Data Image.

From the group of images available for the area selected and identified as B in Figure 5.1 one set of images was chosen to carry out the visual analysis. It consisted of colour composite numbers E-1086-14194 and E-1086-14201 recorded on October 17th 1972. During the interpretation process the black and white 1:1,000,000 transparencies of Bands 5 and 7 were used to support the interpretation. As the objective of this research was to evaluate LANDSAT data as a primary source of information, no references were made during the analysis to the available ground information. The results of the interpretation however, were compared later on with the work produced by DIACA C.A (1958)

and Comerma and Luque (1971).

The first step was the identification of the image classes based on normal photointerpretation procedures. The process was carried out using regular magnifying glasses (8X) and a Baush and Lomb Zoom 240R Stereoscope and the Richards Light Table. From this stage a map shown in Figure 5.2 was produced depicting the classes occurring within the two basins selected.

During this process six classes were found and they were identified as follows:

Class 1. This class includes black and blue areas of smooth texture, representing open standing water (lakes and pounds) and rivers. The black and dark tones are mainly due to the high absorption of infrared energy by water. To obtain better discrimination of the water bodies, a check was made using B Band 7 (.8 to 1.1 μm) in which water has its most characteristic spectral response.

Class 2. This spectrally distinct class has surfaces displaying very light tones and smooth to medium texture. In some cases this class has linear or irregular forms corresponding to fossil sand dunes and sand fields.

Class 3. Areas depicting pale blue to blue-brownish tones and medium texture were delineated in this class. These areas are bare ground (blue tones) and areas with very little vegetation cover. Frequently they represent areas that have previously been burned (blue-brownish).

Figure 5.2 Visual interpretation of LANDSAT image colour composites E-1086-14194 and E-1086-14201 recorded on October 17, 1972

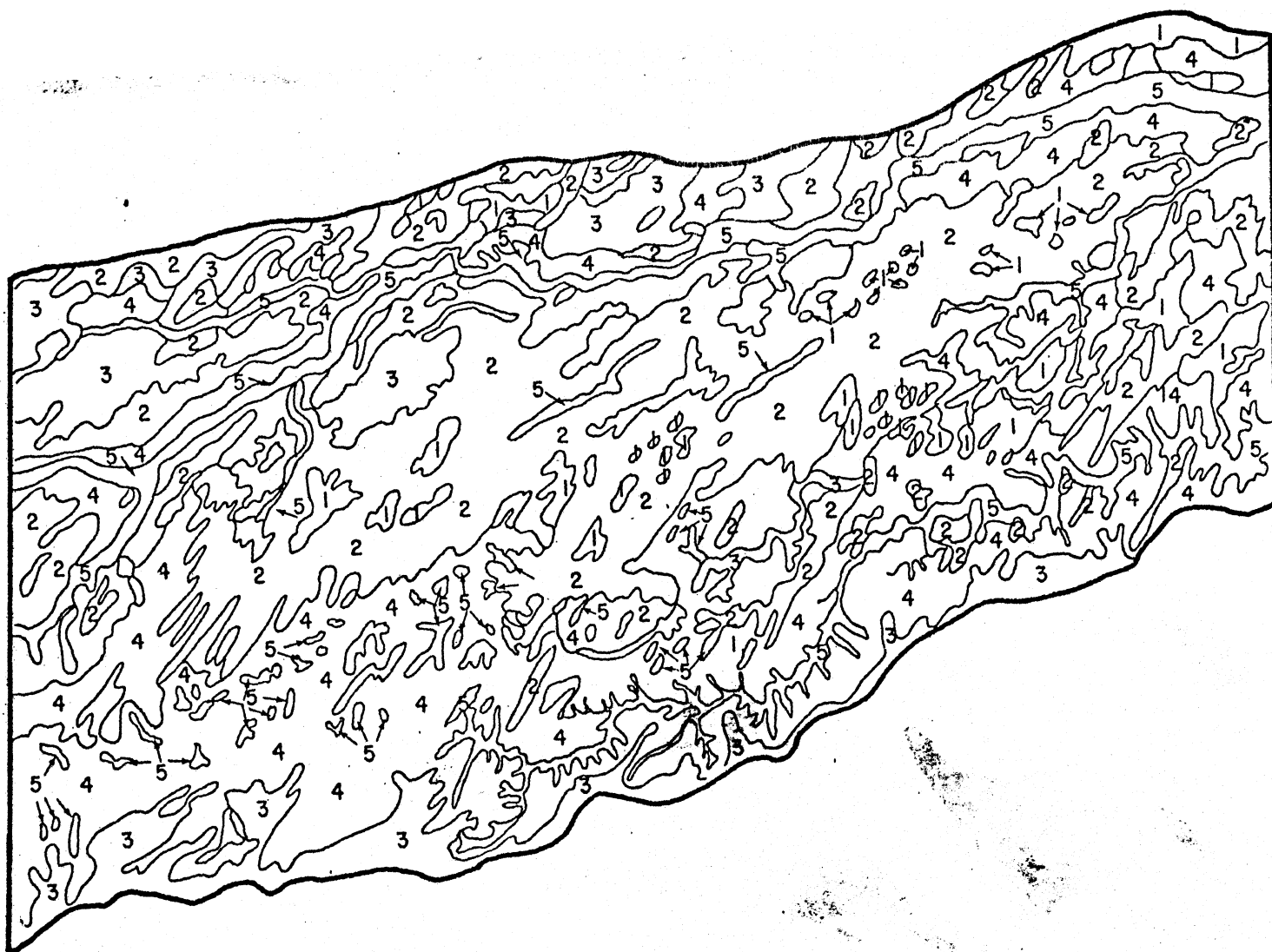


Figure 5.2 Visual interpretation of LANDSAT image, colour composites E-1086-14194 and E-1086-14201 recorded on October 17, 1972.

For description of the classes visually interpreted, refer to pages 59 and 61.

Class 4. Areas showing a brown-red tone and medium to coarse texture. They represent areas with grass cover and occasional shrubs and small trees.

Class 5. This class includes areas with light to dark red tones and medium to coarse texture. Such areas correspond to dense vegetation mainly along the rivers (gallery forest) and small areas on the Plains.

Class 6. This class was represented in the images by dark tones but with a medium texture indicating burned areas.

All six classes can be considered as fairly homogeneous, although a more careful analysis shows that there are several transitional classes and sub-classes within those already identified. With the limitations imposed by the size of the area that can be cartographically displayed (4mm^2), no attempt was made to separate or map them. It must be emphasized however that enlargements at 1:500,000 and 1:250,000 scale may be used as an image base for more detailed mapping.

The information that can be gathered about soil characteristics from LANDSAT visual analysis can only be inferred from landforms, vegetation cover and spectral reflectance characteristics. In Figure 5.3 the map produced is presented, and can be compared with Figure 5.4, in which the information from DIACA C.A (1958) and Comerma and Luque (1971) were integrated. The visual interpretation of the images of Cinaruco and Capanaparo basins was performed in 16 hours.

The results of the visual analysis particularly in land use/land cover suggest that digital analysis can perhaps provide more detail-

Figure 5.3 Soil interpretation using LANDSAT, colour composites E-1086-14194 and E-1086-14201 recorded on October 17, 1972.

1. Gentle rolling terrain with sandy soils.
2. Gentle rolling terrain with sparse sand dunes.
3. Gentle rolling terrain with sparse sand dunes and wide "bajfos".
4. Gentle rolling terrain with numerous narrow "bajfos" and sand dunes.
5. Flat terrain with "bajfos"; poor drainage and sand dunes.
6. Flood plain.

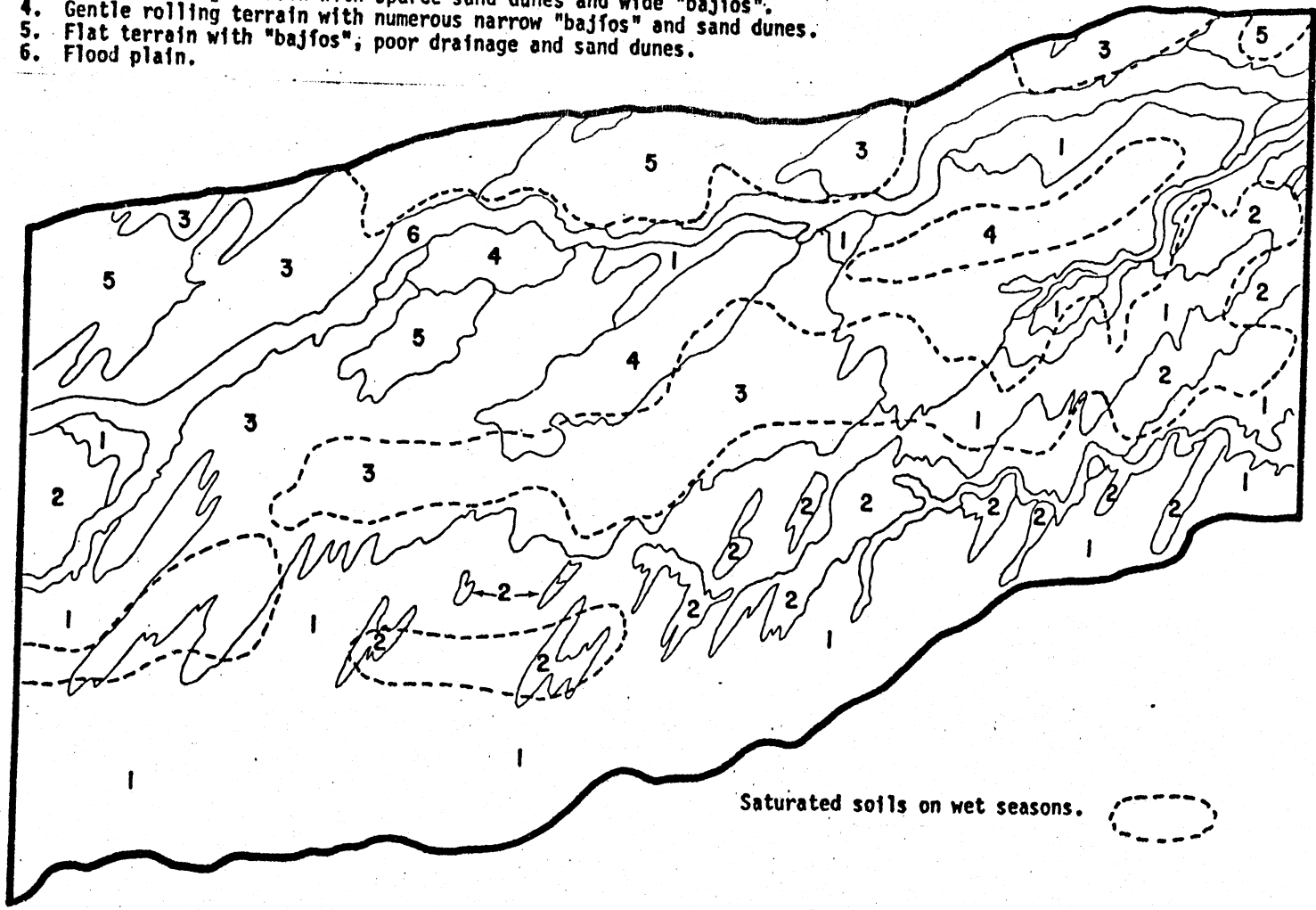


Figure 5.3 Soils interpretation using LANDSAT colour composites E-1086-14194 and E-1086-14201 recorded on October 17, 1972.

ed information.

5.2.3 Landsat Temporal Analysis.

The objective of this part of the research was to evaluate multitime LANDSAT data for monitoring environmental changes. Emphasis was given particularly to: (1) Vegetation cover (seasonal changes and effect of fire), (2) Surface water, and (3) Soil moisture variations (upper zone). To carry out this evaluation two images of the Capanaparo and Cinaruco river basins representing DRY and WET conditions were selected.

Two approaches were used to test the LANDSAT data: (1) Regular visual analysis following the technique already discussed in section 5.2.1 and (2) Density slicing.

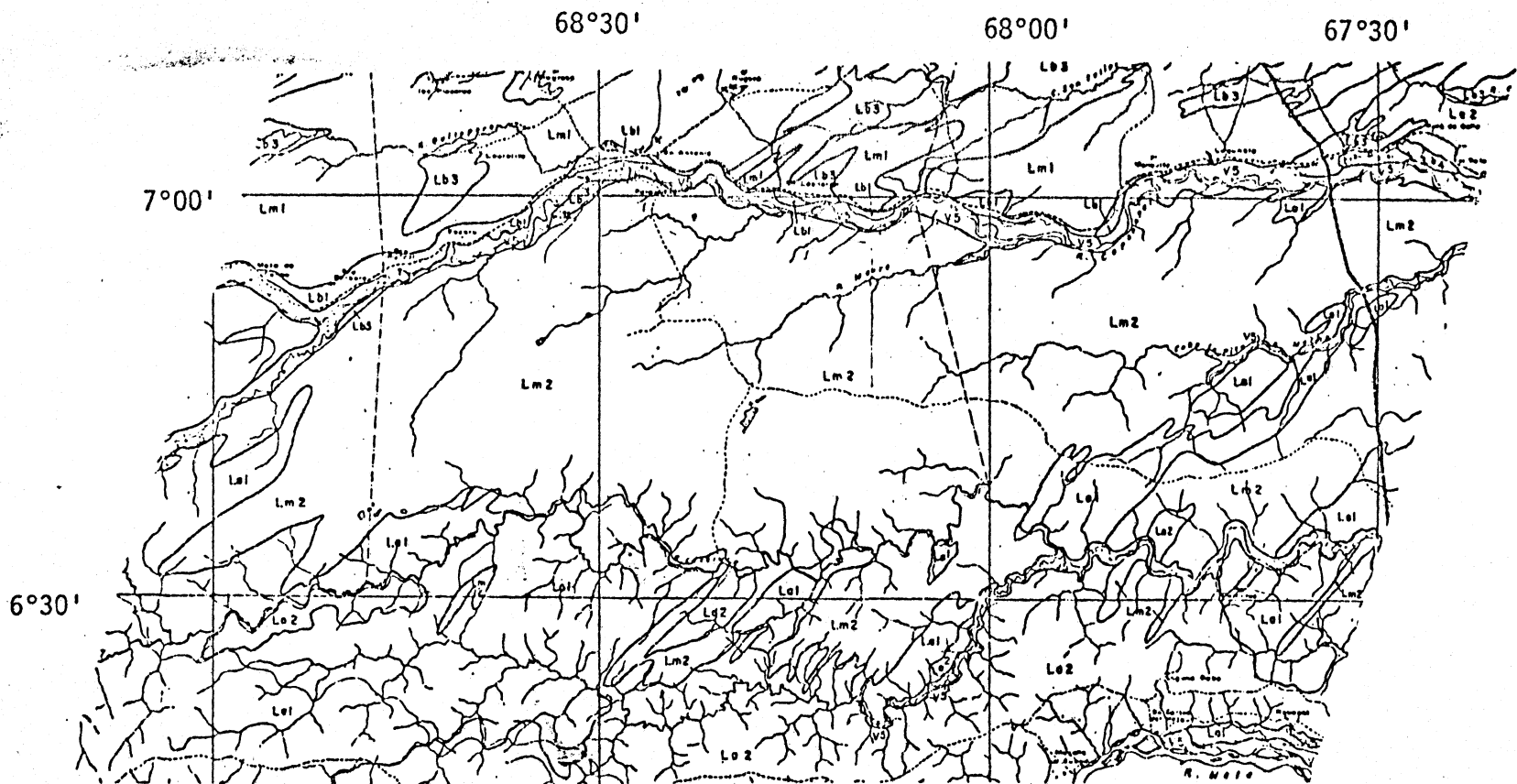
Visual Analysis

In the previous section the result of the visual analysis performed with the images of October 17th 1972 was presented. The imagery used in that case was recorded two months after the peak of the rainy season. The imagery used in this section was recorded on March 10th 1973 (peak of the dry season). Unfortunately no image was available for the southern portion of the area.

In Figure 5.5 the map produced from the interpretation is presented. From a comparison of the two visual analyses, several conclusions can be drawn:

- (1) An increase of bare surface is apparent on the image recorded on March 10th. This is due to a decrease in

Figure 5.4 Soil map of the study area



La1: Gentle rolling terrain. Sandy soils.
 La2: Gentle rolling terrain. Sandy soils with latherite.
 Lb1 and Lb2: Flat terrain with "bajfos" and poor drainage.
 Lb3 and Lb4: Flat and gentle rolling terrain with "bajfos" and "esteros", as well as small areas of sand dunes.

Lm1 and Lm2: Gentle rolling terrain with sand dunes. Areas designated as Lm1 have wide "bajfos", and Lm2 narrow ones.

V5: Flood plain.

Figure 5.4 Soil map of the study area. Scale 1:1,000,000 Source: DIACA (1958).

Figure 5.5 Visual interpretation of image taken on March 10, 1973.

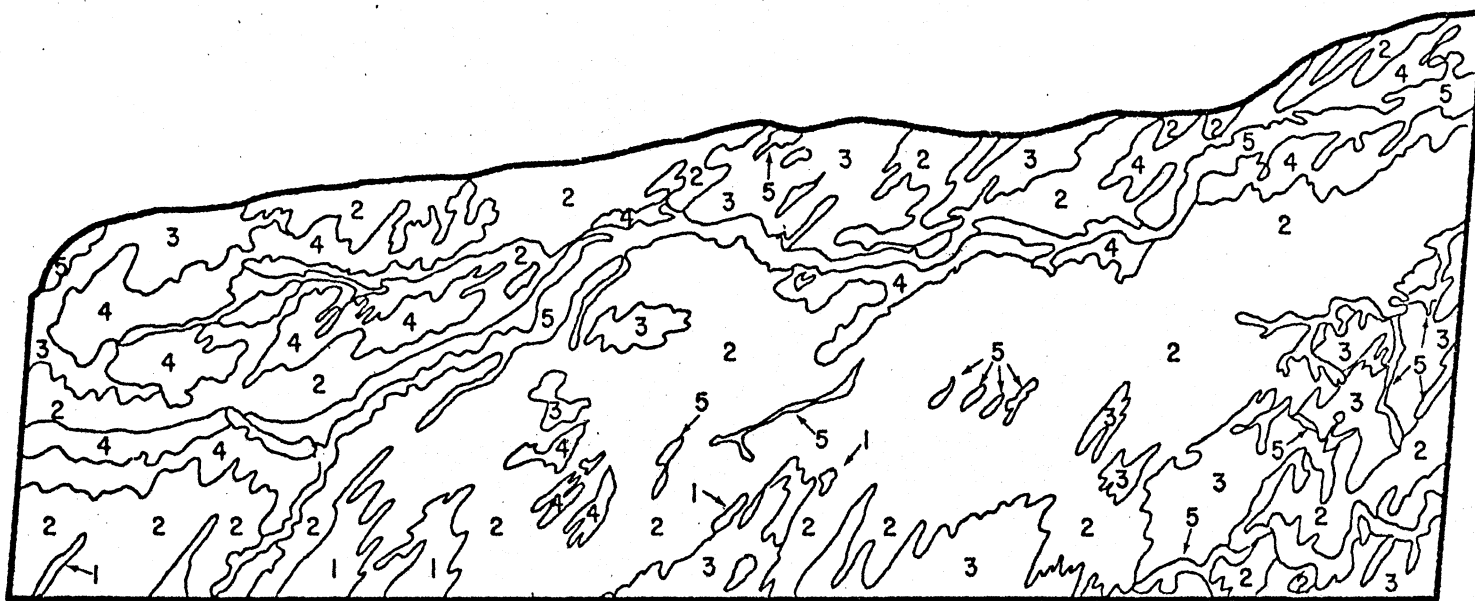


Figure 5.5 Visual interpretation of image taken on March 10, 1973.

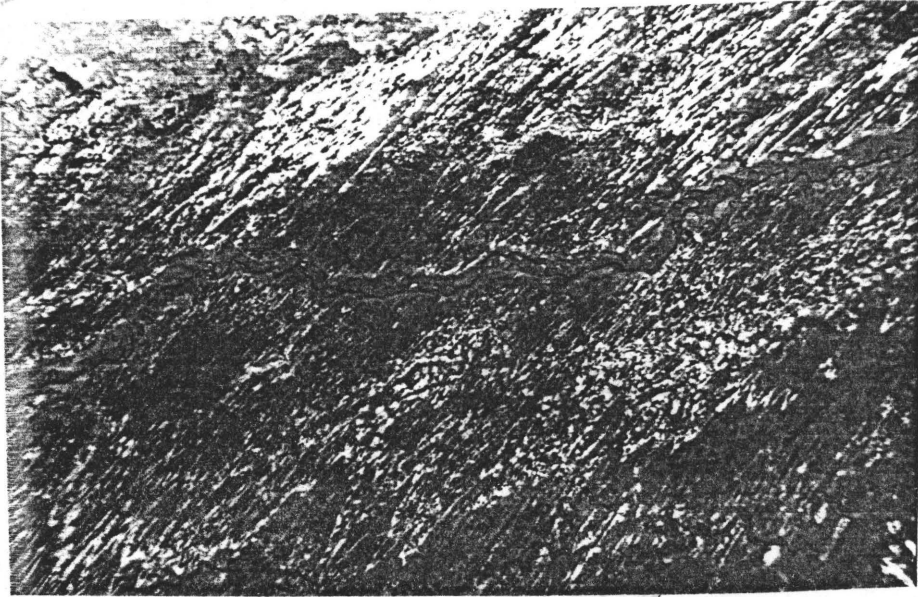
For description of the classes visually interpreted, refer to pages 59 and 61.

vegetation cover that in turn results in a decrease of spectral reflectance, particularly in the infrared spectral region (diminishing the red shade in the colour composite). Although, some sectors are still showing vegetation response, this is mainly along the rivers where the water supply is more stable even during the DRY season.

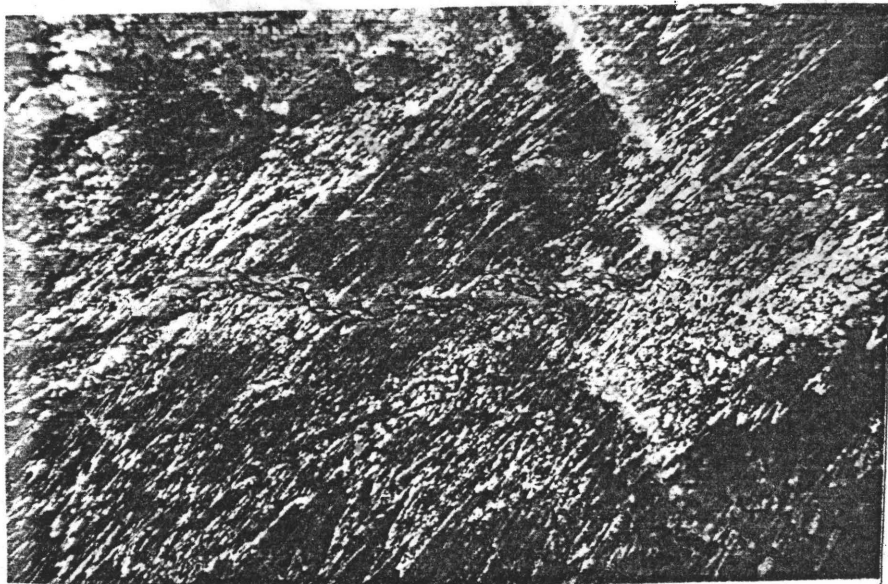
- (2) Changes in the area of surface water are easily observed. The contrast between the DRY and WET seasons is particularly important on the Capanaparo basin. The basin has a large area covered by sand dunes and sand fields. One might think that this area will have no water stored at the surface due to the high infiltration characteristic of sandy soils. It was found by Comerma and Luque (1971), however that very heavy soils were developed in between these sand dunes. This allows the storage of water for fairly long periods of time (3 months).

In the image recorded on March 10, 1973 (maxima of DRY season) none of the water bodies observed on October 17, 1972 can be seen. However, some depressed areas which were occupied by water on October 1972 showed tonal characteristics (browinish -red shade in the colour composite) of vegetation as can be observed at locations A and B in Figure 5.6. The occurrence of vegetation in those areas and no in others can only be explained by the existence of some moisture in the soil, condition no

Figure 5.6 Variations in surface water bodies.



LANDSAT image 1086-14194 recorded on October 17, 1972.



LANDSAT image 1230-14203 recorded on March 10, 1973.

Figure 5.6 Variations in surface water bodies and vegetation cover.

apparent in the surrounding areas.

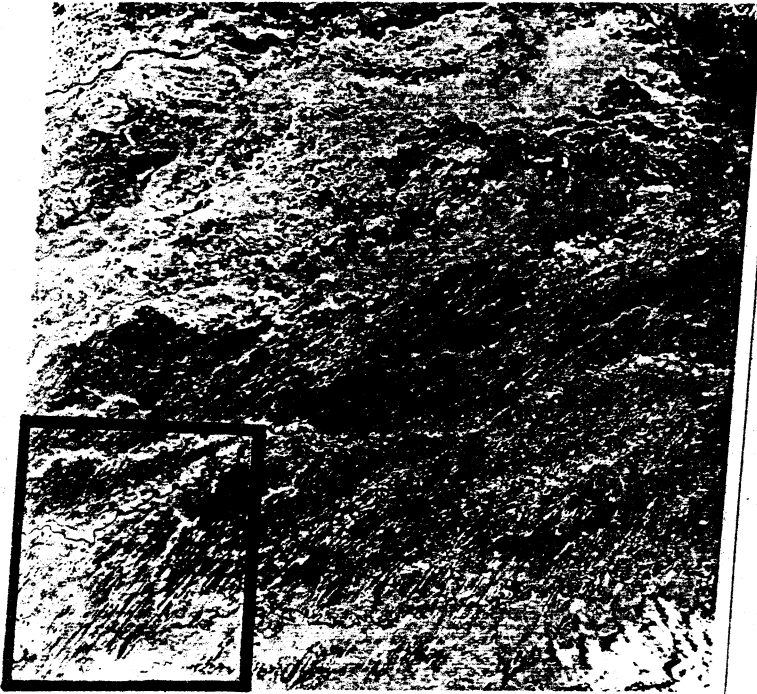
- (3) Due to the characteristic spectral response (low reflectance), saturated soils can be easily observed using LANDSAT Band 7 (.8 to 1.1 μm). Soil moisture, regional as well as seasonal variations can be monitored on the study area because the vegetation is not dense. In most of the cases vegetation reflects the changes in soil moisture.

Density Slicing.

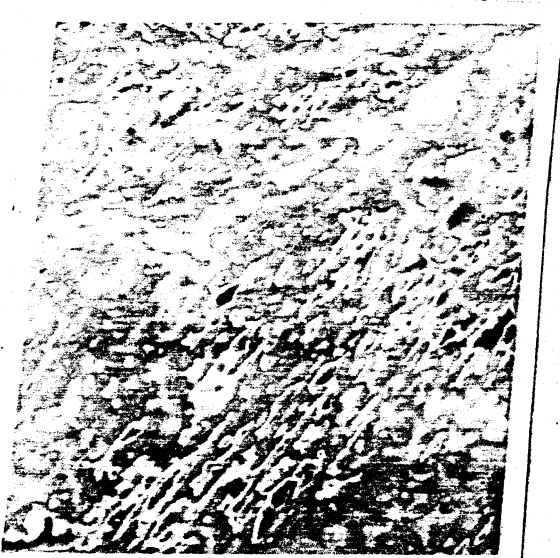
Visual analysis is based on spectral and spatial information. In some cases, however, the differentiation between classes is difficult, particularly if their tonal characteristics are very similar. A density slicer is used for studying density variations in a single image. The instrument separates different gray levels and assigns to them different colours. Therefore tone identification is changed to hue discrimination (Alföldi, 1975). It is important to emphasize that the meaning or environmental significance of each one of the assigned colours has to be established by the interpreter.

Problems were encountered during the density slicing process, being the inconsistencies in the quality of the photographic products the major one. Despite this limitation some attempts were made and good results were obtained when the features identified were spectrally distinct from their background, like water and sand. The result of one case study is presented in Figures 5.7 and 5.8. This material was obtained through the density slicer at the Canada Centre for Remote

Figure 5.7 Density slicing of LANDSAT image: Case A



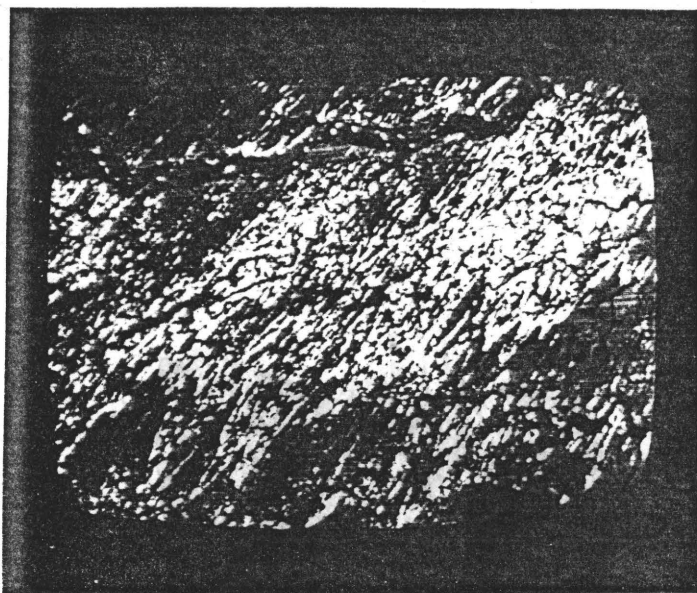
LANDSAT IMAGE 1086-14194 taken on October 17, 1972



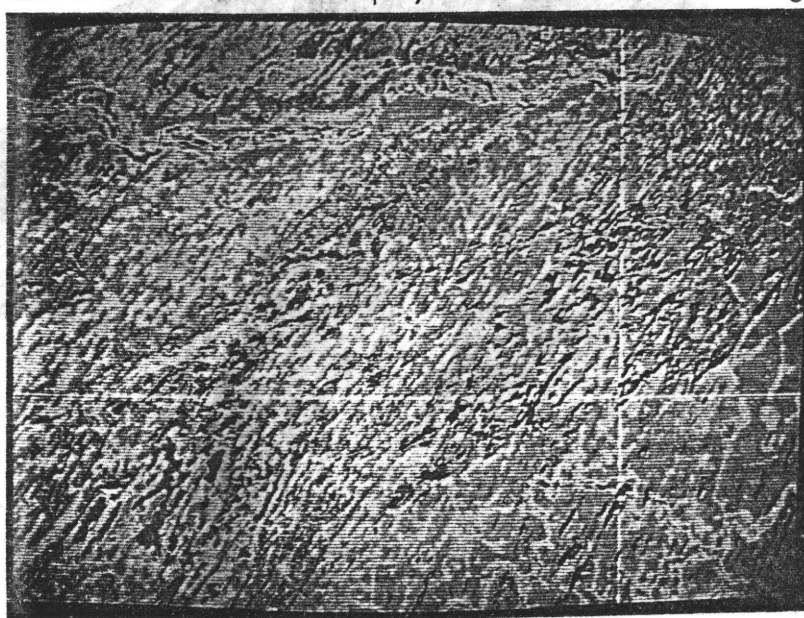
Density level corresponding to water and wet soils

Figure 5.7 Density slicing of LANDSAT image: Case A

Figure 5.8 Density slicing of LANDSAT image : Case B



Black and white monitor display of October 17, 1972 image.



Color display of October 17, 1972 image.

Blue, light blue and green: sand dunes and sand fields.

Light brown: grass and shrubs.

Yellow: tall shrubs, dense vegetation (gallery forest) and wet soils.

Red: Water and saturated soils.

Figure 5.8 Density slicing of LANDSAT image : Case B

Sensing.

5.3 Digital Analysis of Landsat Data.

A computer compatible tape of image E-2029-14142 recorded on February 20 , 1975 by LANDSAT-2 was used in the digital analysis. The amount of information stored in each one of the LANDSAT scenes is 7.5×10^6 four dimensional vectors. If the information required has to be obtained at the limits of resolution, it can only be extracted using digital systems.

Due to the size of the area to be analyzed, it was decided to select test areas. These were identified as MAT-1, MAT-2, MAT-3 and MAT-4, named after the study area (Figure 5.9). All the areas covered 512×512 pixels (40 x 28 Km). The classification procedures were applied to MAT-1 to generate the signatures files, which were later extended to the rest of the areas and finally applied to the whole scene.

5.3.1 Systems for Analyzing Landsat Digital Data.

For processing and extracting information from LANDSAT digital data, several systems have been developed. The General Electric Image 100 and the Bendix MAD systems are the most widely used.

The characteristics of the Image 100 system at the Canada Centre for Remote Sensing (CCRS) and used in this research are given in Table 5. I and Figure 5. 10 .

After the tapes are loaded on the Image 100, the data can be stored in 512×512 pixels sections in the refresh memory (Alföldi, 1975). Up to three of four bands can be displayed at one time, to

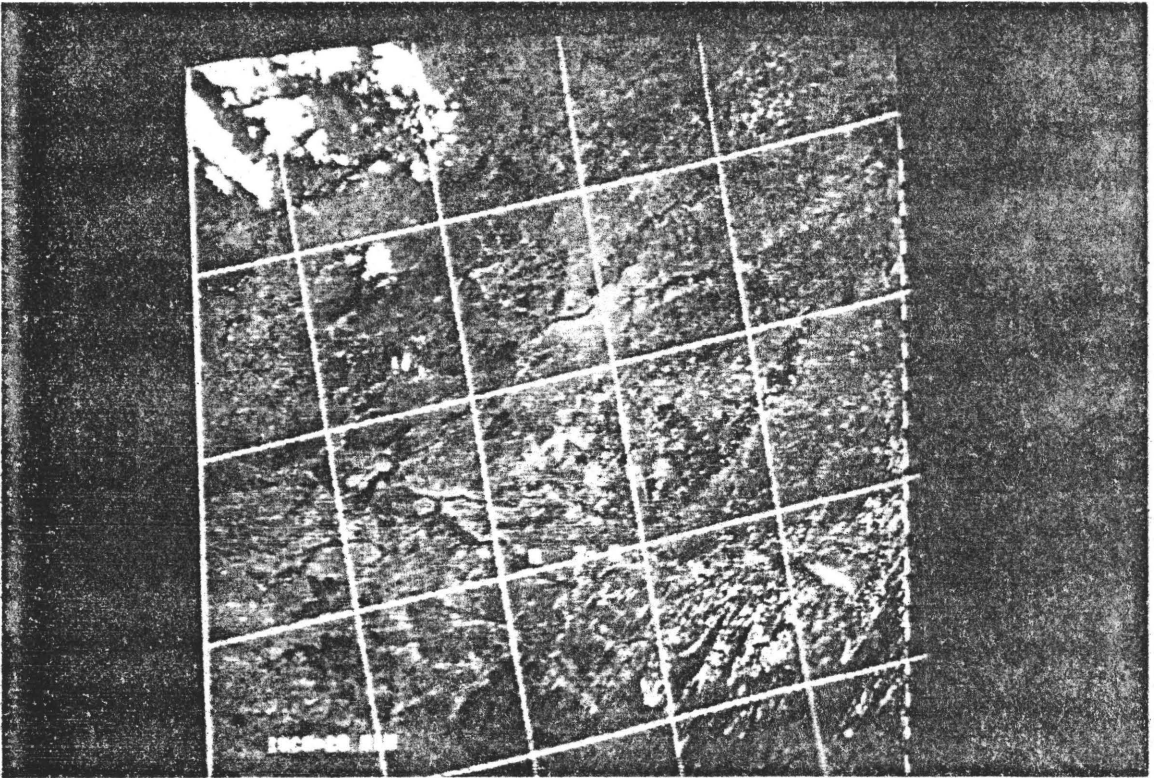


Figure 5.9 Location of the test areas MAT-1
MAT-2, MAT-3 and MAT-4.

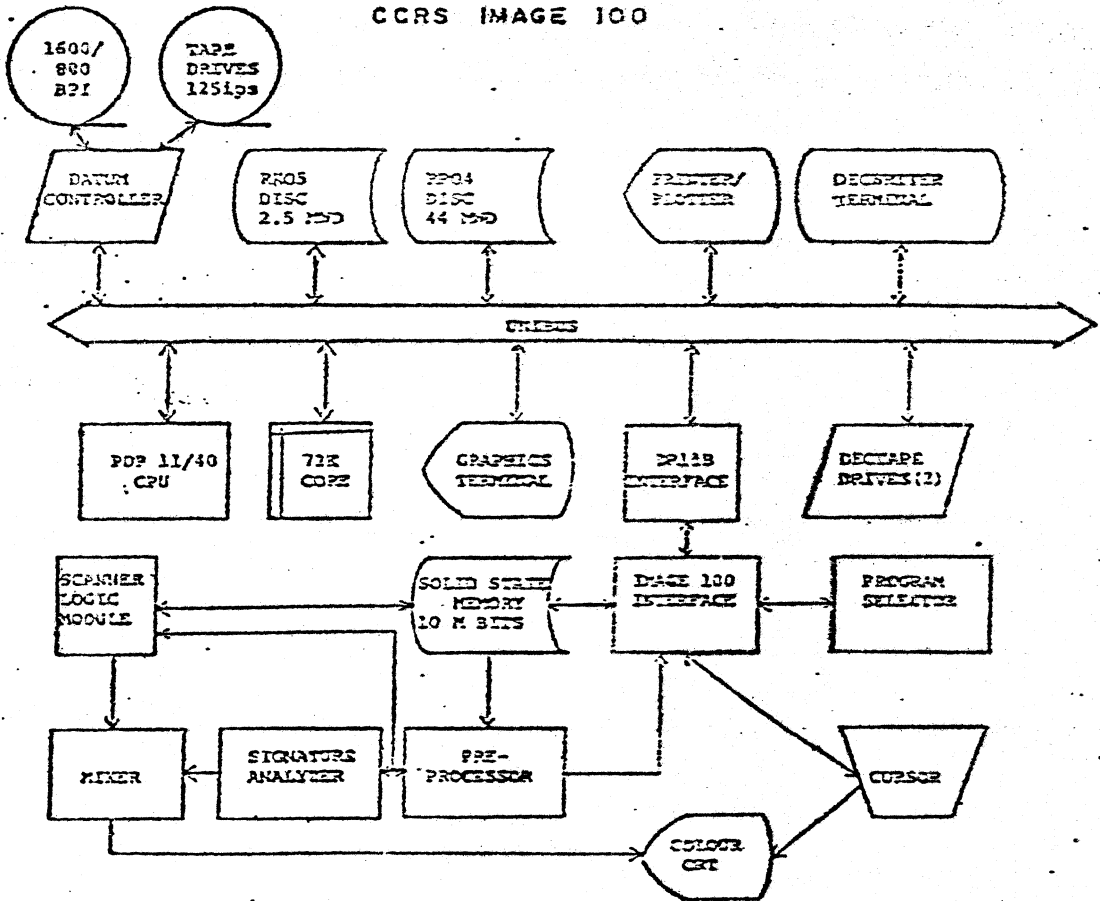
TABLE 5.1

IMAGE 100 CHARACTERISTICS

| | |
|----------------|--|
| COMPUTER : | PDP 11/40 within the system |
| OPERATOR : | Assigned |
| INPUT : | Two tapes drives, and the memory to feed the image into the CRT. |
| DISPLAY UNIT : | Colour T.V. Screen (CRT). Eight themes (8). Cursor with varied size and shape. |
| CONTROL UNIT : | Two units:1.Digital processing logic unit used to select several functions to carried out the analysis of the data. 2.Tektronix display unit, is used in selecting programmes to operate the system. Also displays statistical results. |
| OUTPUT : | 1. Copies of the Tektronix products. 2. Gould Printer (scaled or unscaled) 3. Tapes to be processed via EBIR. 4. CRT display. |

based on Howarth (1976)

CCRS IMAGE 100



Source: Goodenough (1976) p. 19

Figure 5.10 IMAGE 100 System.

produce colour composites. The four channels can also be displayed one by one in black and white on the Cathode Ray Tube (CRT).

The system is capable of performing several enhancement (pre-processing) such as ratioing, normalization, spectral transformation such as principal components and contrast stretching. None of these techniques is considered a classification procedure, although they can be of great help during the classification process. Outputs of these procedures can be obtained through any of the output units (Gould print, Line printer and CRT).

One of the previously mentioned technique called breakpoint was used to make subtle tonal differences in the original scene more obvious. This method was applied to Band 7 to differentiate burned areas. The result of the enhancement is shown in Figure 5.11 . By using this technique three conditions within the burned areas were detected. In Figure 5.11 the three areas delineated correspond to:

- (1) Recent burned areas (note the smoke plume),
- (2) Burned areas with vegetation regrowth
- (3) Old burned areas

In Figure 5.12 and 5.13 two colour composites are shown, one using the regular bands and the second one composed of the regular Bands 7 plus Bands 4 and 5 enhanced (contrast stretching). In the second colour composite, it can be observed that the tonal (spectral) differences resulting from vegetation are greatly enhanced (Fig. 5.13)

5.3.2 Digital Analysis Procedures.

These are two procedures for analyzing LANDSAT digital data

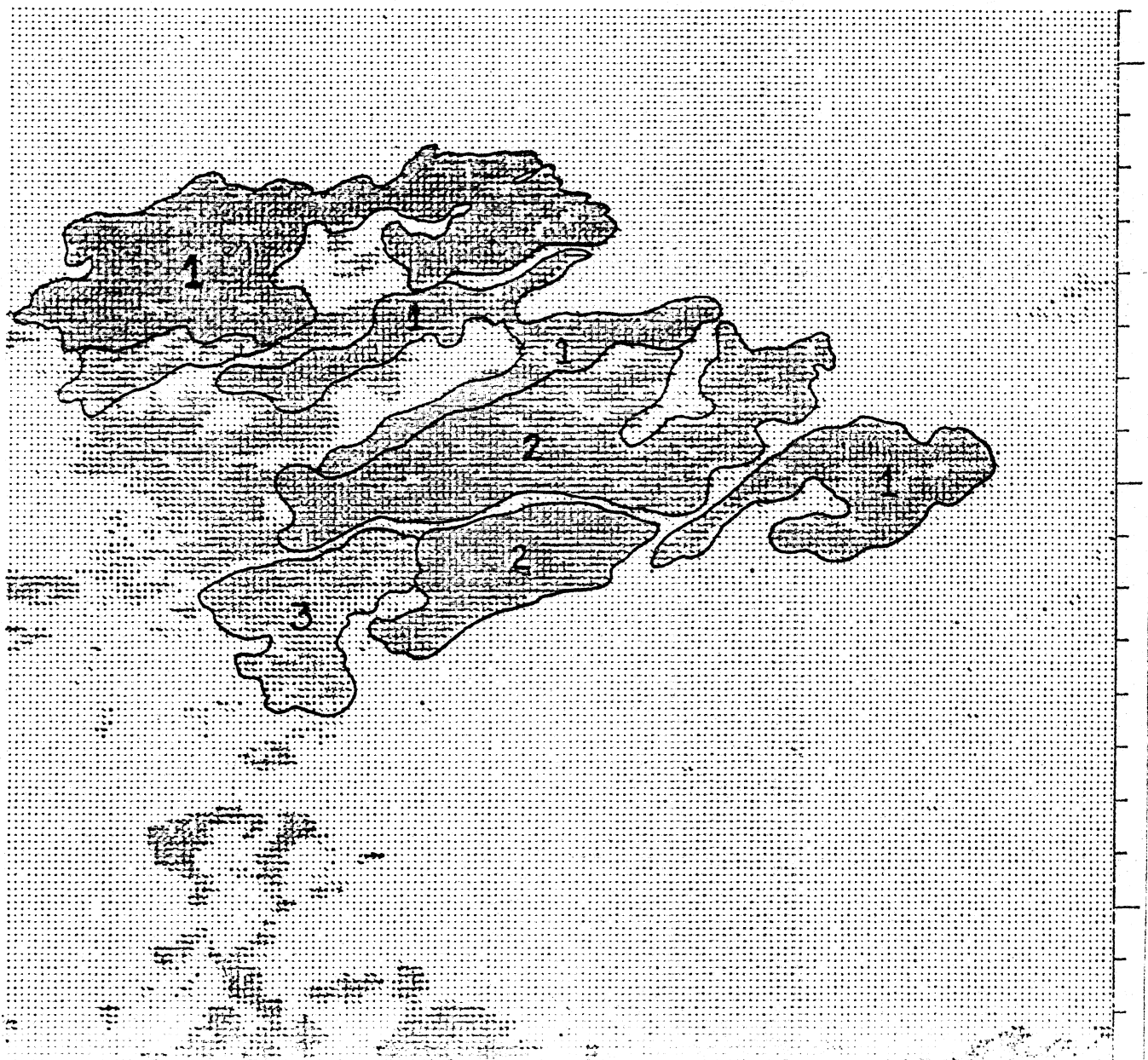


Figure 5.11 Breakpoint enhancement technique: Gould Printer output

(1) Recent burn

(2) Burned areas with vegetation regrowth

(3) Old burned areas

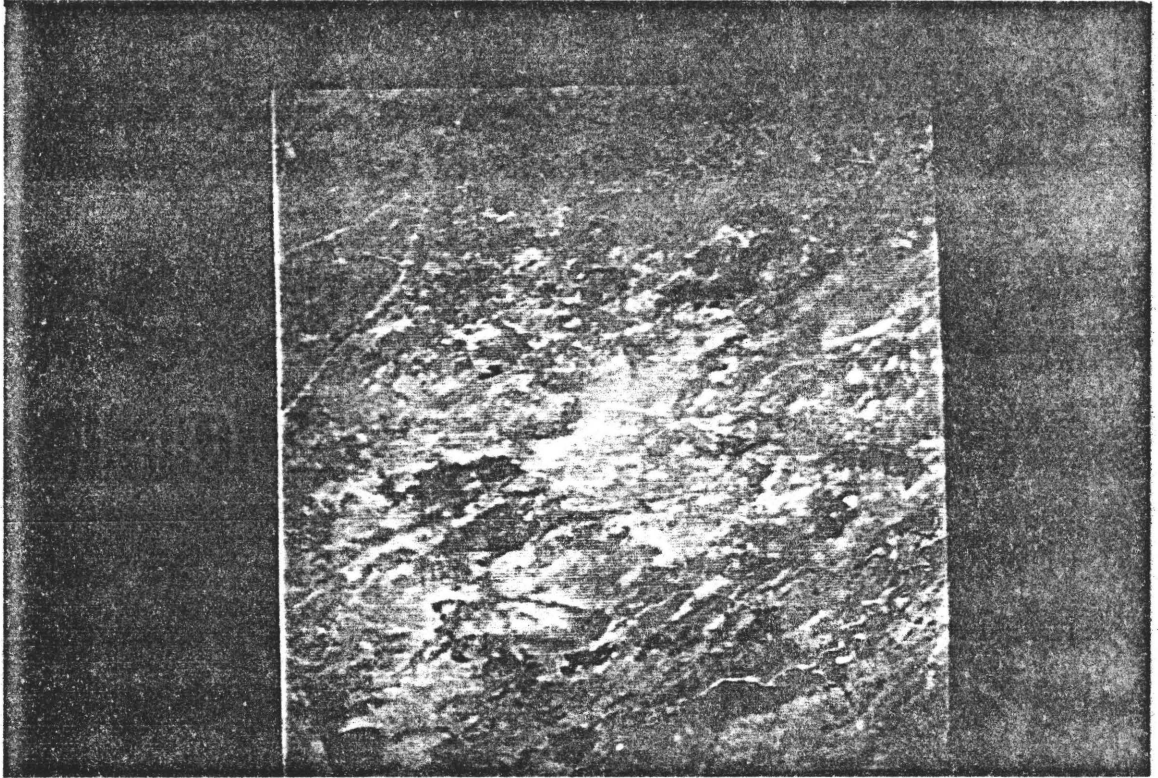


Figure 5.12 Colour composite of Bands 4,5 and 7 displayed on the CRT of the IMAGE 100

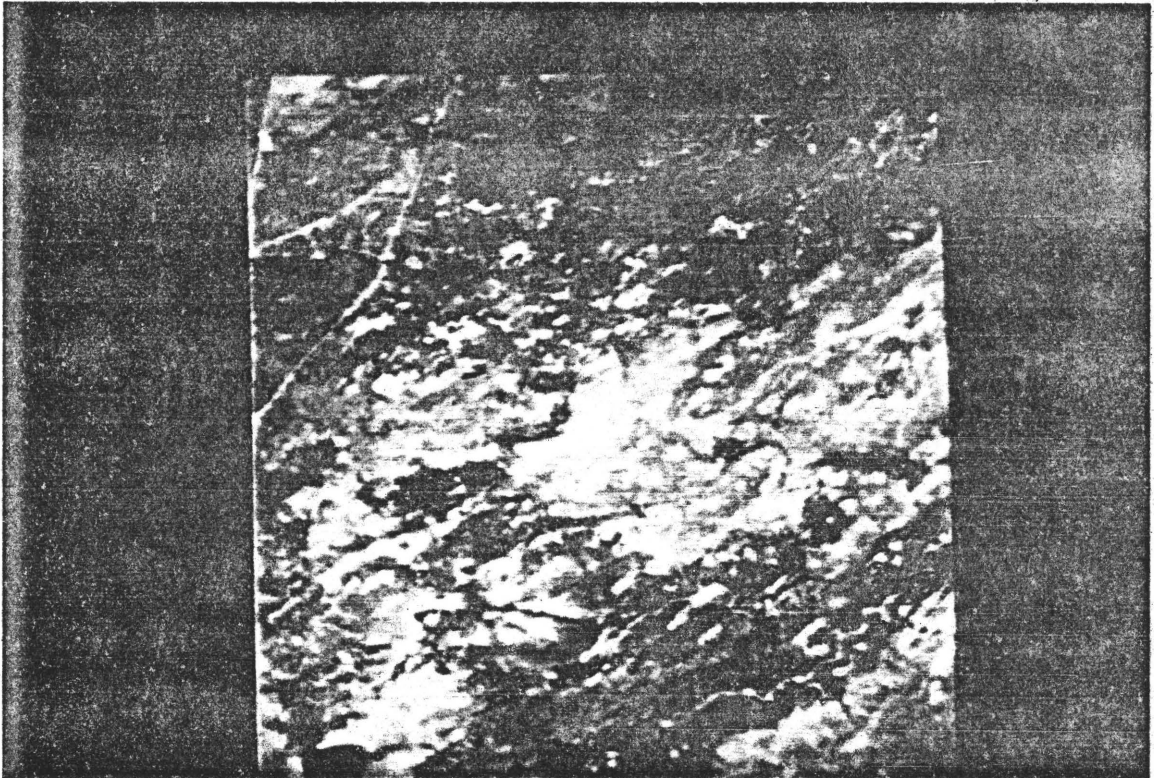


Figure 5.13 Colour composite of Bands 4 and 5 stretched and normal Band 7 produced by the IMAGE 100 (CRT)

namely, unsupervised and supervised classification.

Unsupervised Classification

The unsupervised classification is carried out on the system by establishing statistically valid clusters. A colour is assigned to each one of the clusters and they are displayed on the CRT. The meaning or environmental significance of the individual classes must be established by the interpreter. Several algorithms can be used to perform the unsupervised classification, the Migrating Means and the 4-D Histogram being the most commonly used procedures.

The algorithm used to carry out the unsupervised classification was the Migrating Means. It was applied only to the test area designated as MAT-1. The result of the unsupervised classification is shown in Figure 5.14

The classes obtained in the unsupervised classification were:

Class 1: vegetation, basically gallery forest.

Class 2: vegetation, mainly shrubs.

Class 3: area showing regrowth of vegetation

Class 4: burned areas showing very little vegetation regrow.

Class 5: recent burn

Class 6: grasses 1

Class 7: sandy soils

Class 8: grasses 2

The final unsupervised classification for the test area MAT-1 was filtered using a Nearest Neighbour Algorithm. This algorithm is used to eliminate the isolated pixels giving a "cleaner" appearance

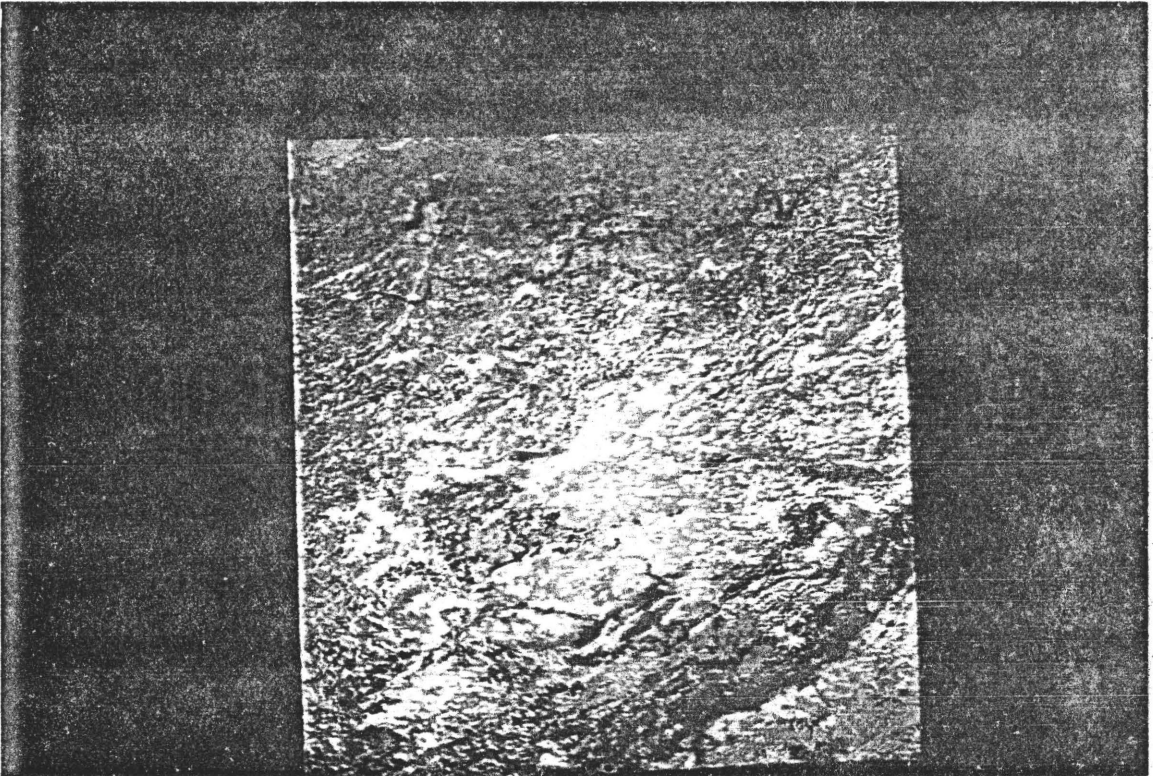


Figure 5.14 Unsupervised classification for
MAT-1 test area

to the final classified scene (Goldberg, 1975). In the present case a 3x3 strong filter was used and the result is shown in Figure 5.15

The signature files used in MAT-1 were saved on tape and then applied to the areas MAT-2, MAT-3 (Figure 5.16) and MAT-4. The final classification of these areas showed that the signature saved can be considered representative of the area displayed by the LANDSAT image. The same signature files were applied to the whole scene and the results were consistent as shown in Table 5.11 . It must be pointed out that this file extension method produce good results in the study area, because of its simplicity. In Figure 5.17 the final unsupervised classification filtered (3x3 strong) for the whole scene is presented.

Supervised Classification

The supervised classification is carried out in an interactive mode. Four steps are generally followed:

- (1) By means of an electronic cursor the user indicates areas on the image that are spectrally different. Those areas (training sets) are selected based on ground information or on the interpreter knowledge about the area.
- (2) The system analyses the spectral properties of the training areas, using a procedure known as "one dimensional signature acquisition" described by Economy et al. (1974)
- (3) All the pixels within the screen which have similar spectral signatures to those selected in the training areas are placed into one class, and displayed as one colour on the CRT.

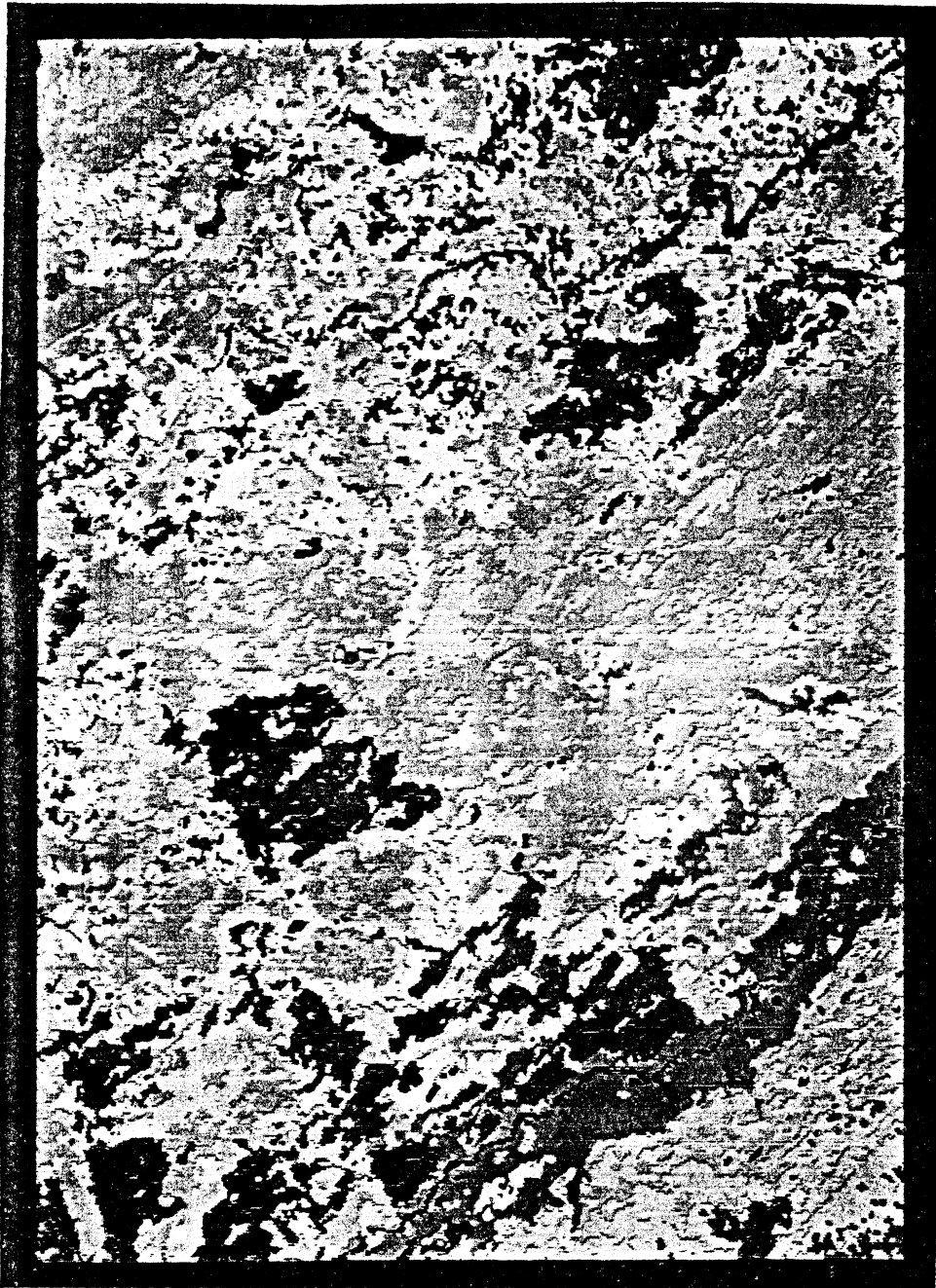


Figure 5.15 Final unsupervised classification produced via EBIR for MAT-1 test area.

| | | | | | |
|-----------|--------------|------------------|-----------|-------------|----------------------|
| Class # 1 | Forest | (<i>lilac</i>) | Class # 5 | Recent burn | (<i>green</i>) |
| Class # 2 | Shrubs | (<i>pink</i>) | Class # 6 | Grasses 1 | (<i>turquoise</i>) |
| Class # 3 | Regrowth | (<i>blue</i>) | Class # 7 | Sandy soils | (<i>beige</i>) |
| Class # 4 | Burned areas | (<i>red</i>) | Class # 8 | Grasses 2 | (<i>yellow</i>) |



Figure 5.16 Final unsupervised classification produced via EBIR for MAT-3 test area, using signatures files created on MAT-1.

| | |
|--|--|
| Class # 1 Forest (<i>lilac</i>) | Class # 5 Recent burn (<i>green</i>) |
| Class # 2 Shrubs, tall grasses (<i>pink</i>) | Class # 6 Grasses 1 (<i>turquoise</i>) |
| Class # 3 Regrowth (<i>blue</i>) | Class # 7 Sandy soils (<i>beige</i>) |
| Class # 4 Burned areas (<i>red</i>) | Class # 8 Grasses 2 (<i>yellow</i>) |

TABLE 5.II

PROPORTION OF EACH CLASS DISPLAYED IN THE FOUR STUDY AREAS (MAT-1, MAT-2, MAT-3 AND MAT-4) AND THE TOTAL SCENE (%)

| CLASS | MAT-1 | MAT-2 | MAT-3 | MAT-4 | TOTAL SCENE |
|--------------|-------|-------|-------|-------|-------------|
| 1 | 1.87 | 0.56 | 3.78 | 7.37 | 2.88 |
| 2 | 3.87 | 2.34 | 5.14 | 8.35 | 5.79 |
| 3 | 7.77 | 5.51 | 15.89 | 28.91 | 13.54 |
| 4 | 14.39 | 14.79 | 24.03 | 31.38 | 20.84 |
| 5 | 17.85 | 4.02 | 7.07 | 5.91 | 6.11 |
| 6 | 28.96 | 33.02 | 13.78 | 7.70 | 18.81 |
| 7 | 9.77 | 1.25 | 3.36 | 2.10 | 3.88 |
| 8 | 12.17 | 28.71 | 9.36 | 2.28 | 12.90 |
| CLASSIFIED | 96.65 | 90.20 | 82.41 | 94.00 | 84.75 |
| UNCLASSIFIED | 3.35 | 9.80 | 17.59 | 6.00 | 15.25 |

NOTE: The low proportion of unclassified pixels in each case indicating good signature file extension. The relatively large percentage of unclassified pixels in MAT-3 and total scene, is due to the occurrence of classes (sand-dunes and clouds) not present in MAT-1 (Figures 5.16 and 5.17).

Figure 5.17 Final unsupervised classification produced via EBIR for the LANDSAT scene E-2029-14142.

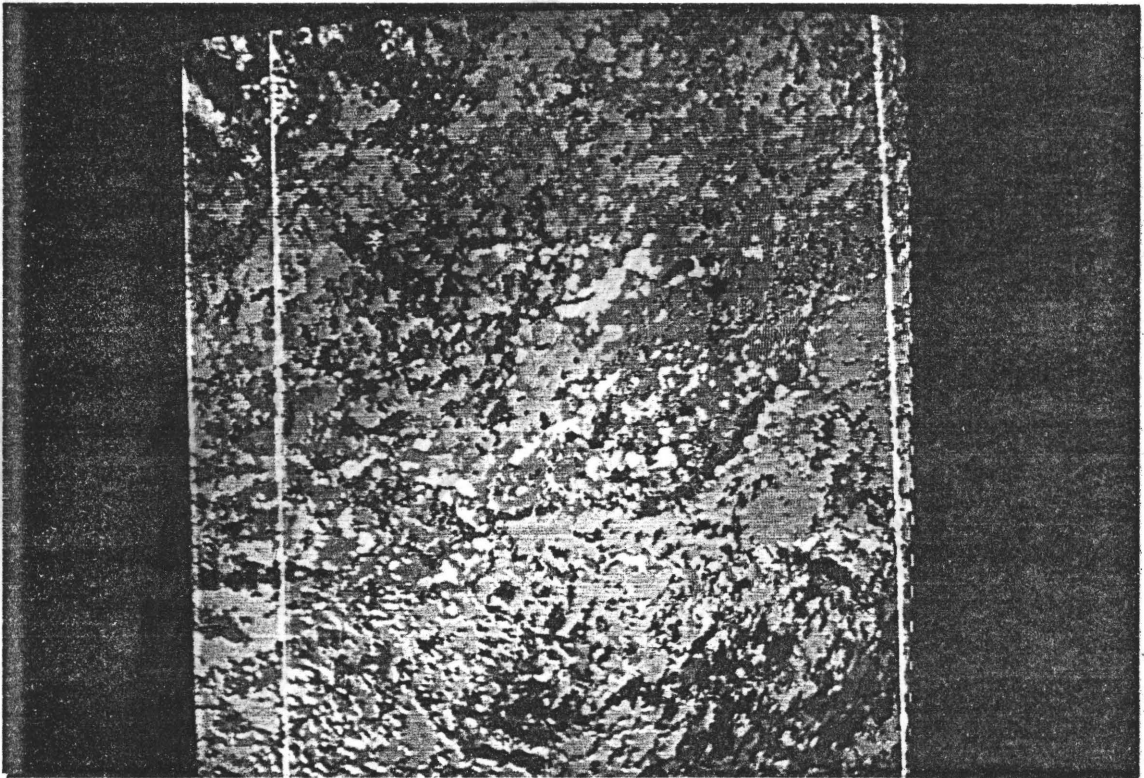


Figure 5.17 Final unsupervised classification produced via EBIR for the LANDSAT scene E-2029-14142.

- (4) The procedure is repeated for each of the classes identified. When all the classes occurring on the area have identified a maximum of 8 classes may then be displayed on the CRT.

Three types of output can be obtained:

- (1) The photographic output through the Electron Beam Image Recorder (EBIR).
- (2) The line printer (scaled).
- (3) The Gould printer either one theme scaled or all the themes unscaled.

The themes obtained for MAT-1 using the supervised classification were:

Theme # 1: Burned areas.

Theme # 2: Vegetation, shrub.

Theme # 3: Water (clear)

Theme # 4: Grass #1

Theme # 5: Grass #2

The differences between Grass #1 and #2 are mainly due to soil conditions rather than structural or density.

Theme # 6: Water (silty)

Theme # 7: Forest

The final classification is shown in Figure 5.18

5.4 Discussion.

The results show that LANDSAT photographic and digital products can be used for obtaining information on land use/land cover as well as some soil characteristics over large areas.

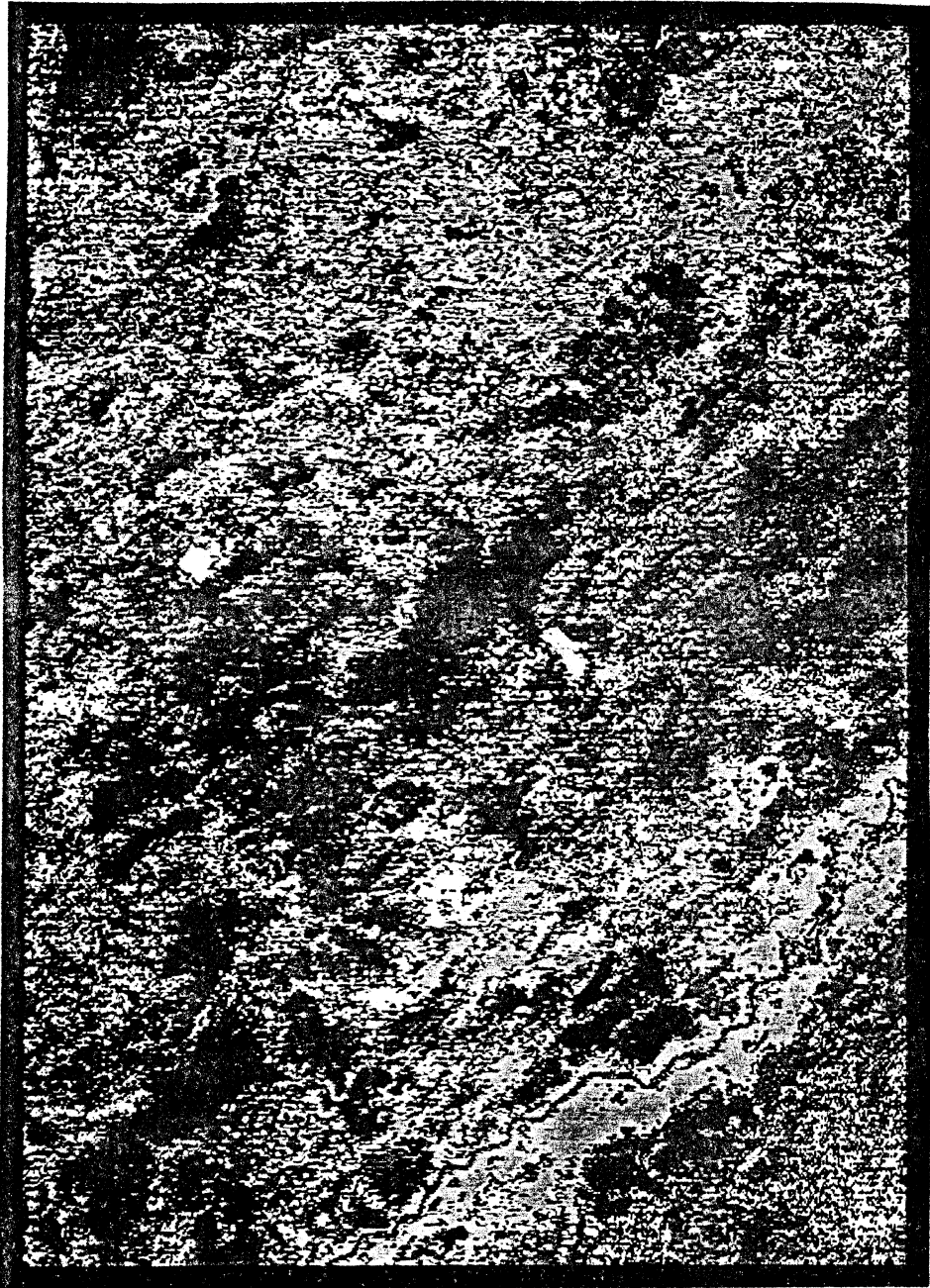


Figure 5.18 Final supervised classification produced via EBIR for MAT-1 test area.

- | | |
|------------------------------------|-----------------------------------|
| Theme # 1 Burned area (green) | Theme # 5 Grass 2 (pink) |
| Theme # 2 Vegetation Shrub(yellow) | Theme # 6 Water silty (turquoise) |
| Theme # 3 Water (clear) (blue) | Theme # 7 Forest (lilac) |
| Theme # 4 Grass 1 (red) | |

Various levels of information can be gathered from LANDSAT data. The visual analysis, although highly dependent on the scale of the image used, produce useful information. Up to six land cover classes were identified in the Cinaruco-Capanaparo basin and the same in the Matiyure basin.

Regarding the results of the digital analysis, the supervised classification for MAT-1 test area produced seven classes, while with the unsupervised eight were identified. The signature files developed in MAT-1 were extended to the whole scene (32,400 km²) and acceptable results were obtained (Table 5.II).

The information extracted using any of the systems of analysis applied can not be used directly in the models. It has to be transformed in order that it can be incorporated into the pertinent equations.

Others have suggested that land use/land cover affect such hydrologic processes as evapotranspiration and infiltration. Many models, particularly those need in urban, agricultural and forest hydrology, considered land use/land cover as a very important elements. One example is the Holtan (1971) infiltration equation expressed as:

$$f = FA \cdot GI \cdot a \cdot Sa^n + f_c$$

where:

f= instantaneous rate of infiltration in inches/hour

FA= a coefficient which together with "a" accounts for the effect of land use types in infiltration.

GI= growth index of plants

Saⁿ=available storage in surface layer of the soil ("A" horizon) in inches of water equivalent.

n = a function of soil texture. For silt $n=1.4$, sand $n = 1.4$
and clay $n = 1.4$

f_c = constant rate of infiltration after prolonged wetting in
inches per hour (f_c is associated with capillary flow or
with an impeding soil stratum)

In Table 5. III values of vegetative parameter "A" are given.

Note that the land use/land cover types numbers 6, 7, 11, 12 and 14 are present in the study area.

For each unit element a weighted average coefficient is computed. This coefficient accounts for the percentage of each land cover/land use class within each unit element.

Several methods can be used to extract that information from the maps produced by the visual analysis or from the outputs of the digital systems.

To extract information from the maps a 1 mm grid overlay is suggested. The information is extracted grid by grid and then coded for location and class.

In the case of the digital analysis the approach will depend on the type of output used. With the EBIR (Fig. 5.17), Gould Printer, scaled or unscaled (Figures 5.19 and 5.20) the system is the same as the one mentioned for the visual analysis. In this case the information is more detailed, because it is processed and displayed at pixel levels. However it must be pointed out that the method is time-consuming.

An alternative approach is to use the output generated by the Line Printer attached to the Image 100. The classes established in the interpretation process are numerically coded (1 to 8) and displayed by

TABLE 5.III

VEGETATIVE PARAMETER "A" IN HOLTAN'S INFILTRATION EQUATION

| <i>NO</i> | <i>LAND USE DESCRIPTION</i> | <i>VEGETATIVE PARAMETER</i> |
|-----------|---------------------------------------|---------------------------------|
| 1 | Crop Land | 0.15 |
| 2 | Urban-built up | 0.05 |
| 3 | Mines, Quarries, Sand and Gravel Pits | 0.2 |
| 4 | Orchards and Vineyards | 0.3 |
| 5 | Horticulture, Fur and Poultry | 0.2 |
| 6* | Rough Grazing and Rangeland | 0.4 |
| 7* | Rock & Other Unvegetated Surfaces | 0.0 |
| 8 | Swamp, Marsh or Bog | 0.0 |
| 9 | Outdoor Recreation | 0.4 |
| 10 | Improved Pasture and Forage Crops | 0.8 |
| 11* | Sand Flats, Dunes and Beaches | 0.8 |
| 12* | Woodland | 0.8 |
| 13 | Non-productive Woodland | 0.7 |
| 14* | Water | 0.0 |

Source: Gupta (1974)p. 211

* Categories present
in the study area.

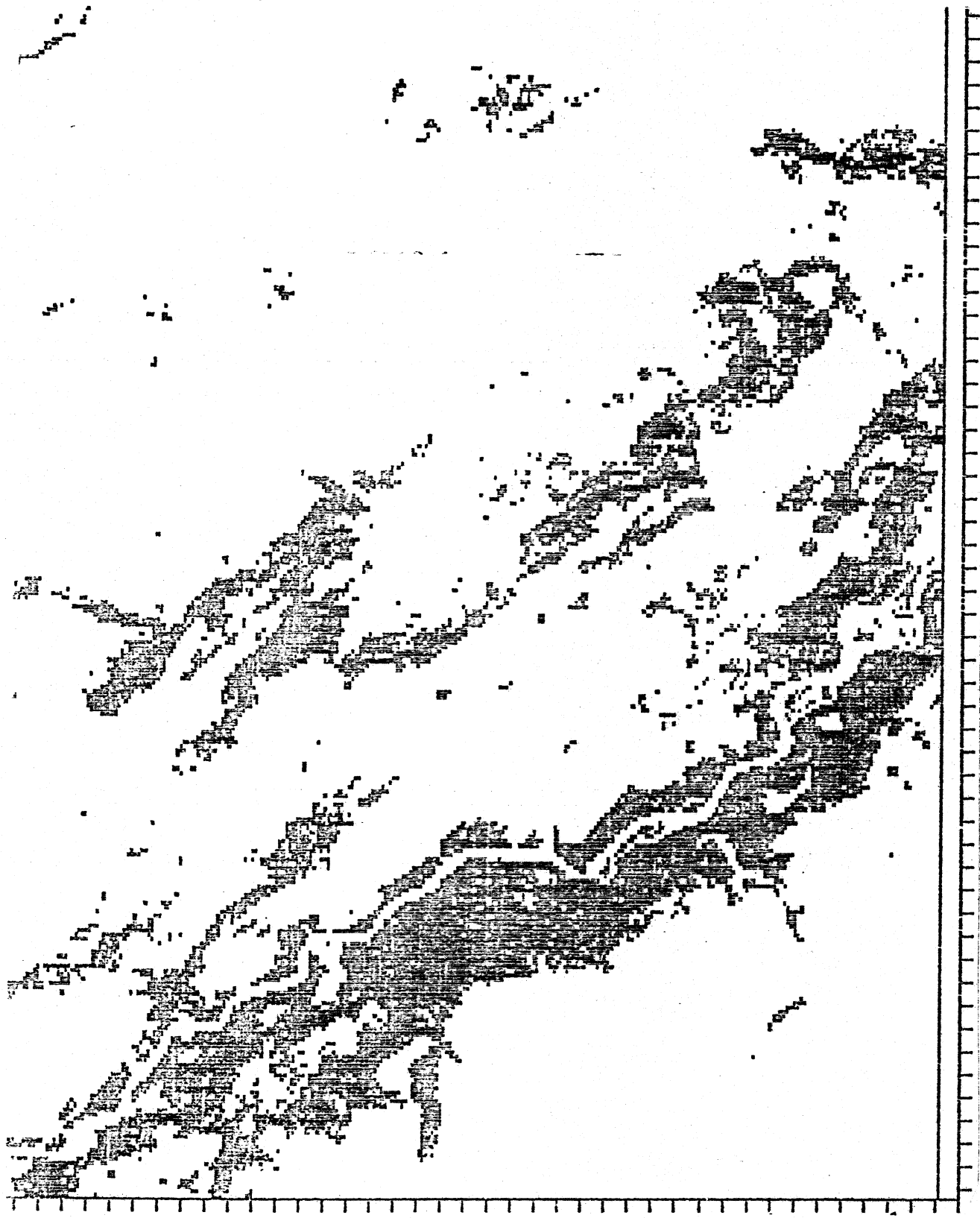


Figure 5.19 Gould Printer unscaled. Themes output of part of MAT-1 of part of MAT-1, unsupervised classification.

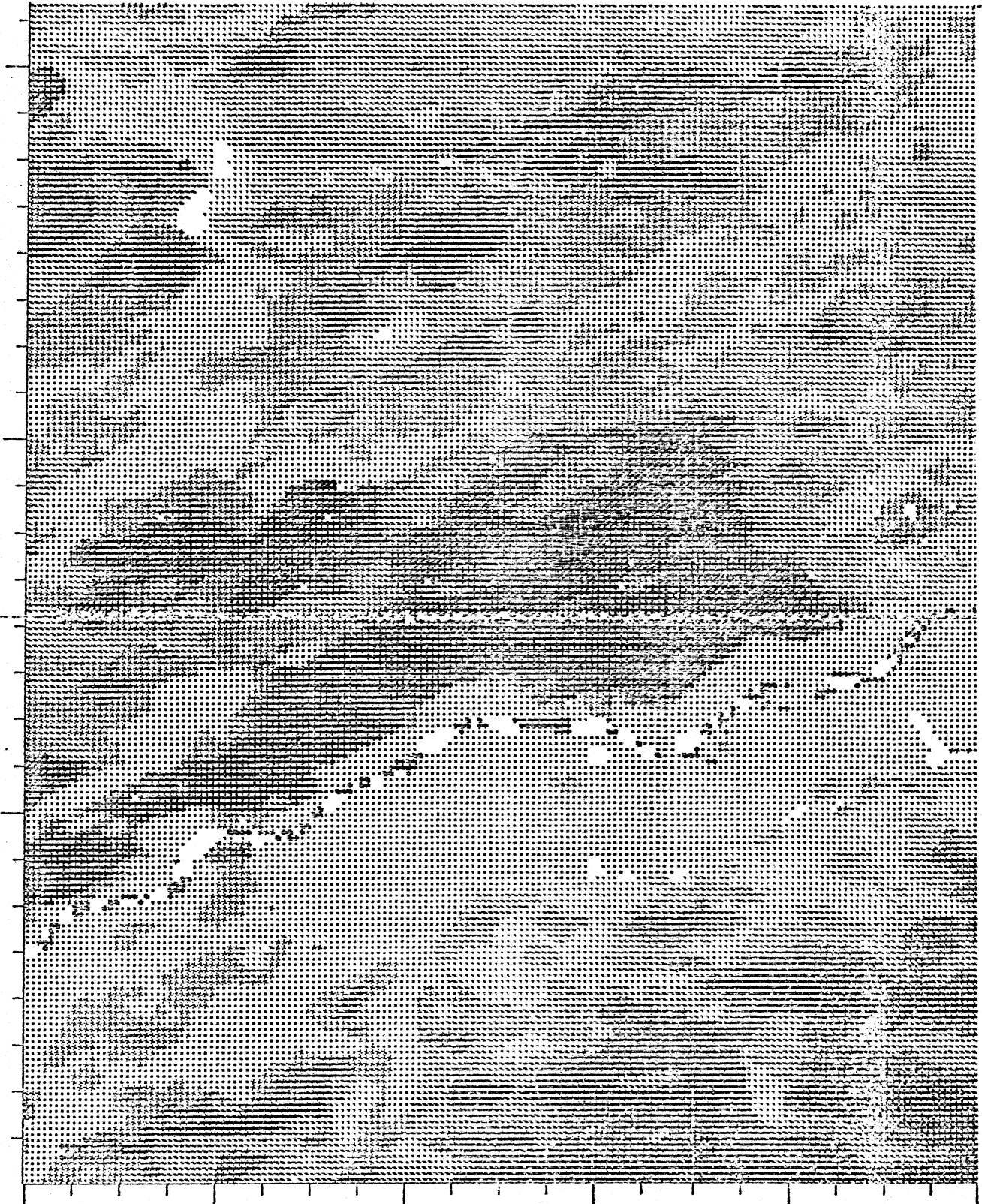


Figure 5.20 Gould Printer unscaled. Themes output of part of MAT-1, unsupervised classification (Forest)

the printer at the scale desired. The character also has its location w_i within the scene coded by line and by pixel number as shown in Figure 5.21. The scale of this output is not as exact as the one from the Gould Printer (Fig. 5.19) because of distortion due to character size. However, Fig. 5.22 shows that both outputs related well. The Line Printer output was also compared with a 1:100,000 topographic map and the result is shown in Fig. 5.23. The number of pixels displayed for each one of the characters is approximately 5.36×4.36 pixels (423x244 m) or an area of 0.103 km^2 . A second output at 1:500,000 was generated from the Line Printer (Fig. 5.24). Although a large amount of information was lost, the general pattern remains the same as shown in Figure 5.21.

Area measurements from the Line Printer output can be made, using a factor of 0.103 km^2 (1:100,000 scale) per character and multiplying by the number of occurrences of the class within the unit element.

In Section 5.2.3 the possibilities of detecting seasonal and non-seasonal changes have been demonstrated. The results suggest that seasonal information could be applied to obtain better estimates of model parameters.

CHAPTER 6

CONCLUSIONS

In recent years the use of hydrologic mathematical models has increased greatly. Distributed mathematical models have been considered an important tool in urban, agricultural and forest hydrology. Their use has always been limited, however, because of the amount of information that they require. Conventional methods used in extracting the information are time-consuming, expensive and limited, particularly when large drainage basins are involved. Remote sensing from spacecrafts such as GOES and LANDSAT can be used as means of gathering part of the information required (namely, precipitation and land use/ land cover), rapidly, repetitively, with an acceptable accuracy in a less expensive way.

GOES data was found useful in improving information on the temporal and areal distribution of precipitation in the study area. The continuous coverage (every 30 minutes) in two spectral bands (visible and thermal infrared) allowed the identification and monitoring of activity of the different types of rain-producing clouds day and night.

Follansbe's (1973) method for estimating precipitation from satellite imagery was selected. Although the method is empirical, it has been tested in several areas of the world, including tropical areas. It has produced satisfactory results in areas where information is dif-

difficult to obtain. Some changes that are required to make it suitable for hydrologic distributed models are proposed. Due to lack of hourly precipitation data for the study area, however, the method could not be tested.

LANDSAT data in its two formats (photographic and digital) was evaluated. The results showed that the level of detail on land use/land cover that is required for hydrologic distributed models can be obtained. It is limited, however, by the type of product used. Visual analysis using single and multirate data allowed the identification and mapping of broad land use/land cover categories as well as soil characteristics. This is possible because in the visual analysis both tone and texture aided identification. Multirate data was found applicable to monitor seasonal as well as non-seasonal changes. The inconsistency in quality of the photographic products, however, limited the use of the density slicing technique, although good results had been expected.

Digitally enhanced data was found valuable for improving visual interpretation. These products could open a feasible way for making the maximum application of both spatial and spectral information used in visual interpretation. Similar results to those produced by digital methods could perhaps be obtained without the high cost involved.

Land-use/land-cover information at the level required for hydrologic distributed models can be obtained by digital analysis using either unsupervised or supervised techniques. In the case of the unsupervised classification more detailed post-interpretation is required.

From this evaluation, it can be concluded that satellite data

from GOES and LANDSAT are powerful tools for obtaining the information required for hydrologic distributed models.

BIBLIOGRAPHY

- Alföldi, T.T., "*The use of satellite imagery for an inventory of Coastal Resources in The Atlantic Provinces*", Research Report 75-5, Canada Centre for Remote Sensing, Ottawa: Department of Energy, Mines and Resources, 1975.
- Ambaruch, R. and J.W Simmons, "Use of continuous simulation models in application of remote sensing to hydrology", Tech. Rept. IBM N^o 732000408 presented at *1973 Summer Computer Simulation Conference*, Montreal, Canada, July 1973.
- Ambaruch, R. and J.W Simmons, "*A study of remote sensing as applied to regional and small watersheds*", Tech. Rept. IBM N^o 74W-00175, Goodard Space Flight Center, June 1974.
- Amorocho, J., "An application of satellite imagery to hydrologic modeling in the Upper Sinú basin, Colombia" in *Symposium and workshop on the application of mathematical models in hydrology and water resources systems*, Bratislavia, 8-13 Sept. 1975.
- Barker, J., "Area measurements of water from Landsat" in *Proceedings of the 10th International Symposium on Remote Sensing of the Environment*, Ann Arbor, Michigan, 1975.
- Barrett, E.C., "*Viewing weather from space*", New York: Frederick A. Praeger, 1967.
- Barrett, E.C., "The estimation of monthly rainfall from satellite data" in *Monthly Weather Review*, 98, 1970, pp. 322-327.
- Barrett, E.C., "Forecasting daily rainfall from satellite data", in *Monthly Weather Review*, 101, 1973, pp. 215-222.
- Clarke, R.T., "A review of some mathematical models used in hydrology, with observations on their calibration and use" in *Journal of Hydrology*, 19, 1973, pp. 1-20.
- Comerma, J.A. and O. Luque, "Los principales suelos y paisajes del Estado Apure" in *Agronomía Tropical*, Vol. XXI, N^o 5, 1971 pp. 379-396.
- Conover, J.H., "*Cloud interpretation from satellite altitude*", Research Note 81, Massachusetts: Air Force Cambridge Research Laboratories, 1962.

- Crawford, H.N. and R.K. Linsley, "Digital simulation in hydrology: Stanford Watershed Model IV", Tech. Rept. 39, Stanford Univ., 1966.
- Desarrollo Industrial Agrícola, C.A., "Mapa de suelos del Estado Apure" (1:500,000), Caracas, 1958.
- Deshler, W., "An examination of the extent of fire in the grassland and savanna of Africa along the southern side of the Sahara" in *Proceedings of the 9th International Symposium on Remote Sensing of the Environment*, Ann Arbor, University of Michigan, 1974, pp. 23-30.
- Economy R.D., D. Goodenough, R. Ryerson and R. Towles, "Classification accuracy of the Image 100" in *Proceedings of the Second Canadian Symposium on Remote Sensing*, Guelph, Ontario, 1974, pp. 277-287.
- Fleming, G.F., "Computer Simulation Techniques in Hydrology", New York: Elsevier, 1975.
- Follansbee, W., "Estimation of average daily rainfall from satellite cloud photographs", NOAA, Tech. Memo. NESS 44, Washington: National Environmental Satellite Service, NOAA, 1973.
- Freeze, R.A., "Blueprint for a physically-based, digitally simulated hydrologic response model", *Journal of Hydrology*, 9, 1969, pp. 237-258.
- Freeze, R.A., "Streamflow generation", in *Review of Geophysics and Space Physics*, Vol. 12, No 4, 1974, pp. 627-642.
- Freile, A.J., "Provincias Fisiográficas de Venezuela", Caracas: Sección Geografía, Ministerio de la Defensa, 1965.
- Freile, A.J., "Regiones Climáticas de Venezuela", *Boletín de Geología*, Vol. X, No 19, Caracas: Ministerio de Minas e Hidrocarburos, 1969.
- Goodenough, D., "Image 100 Classification Methods for ERTS Scanner Data", in *Canada Journal of Remote Sensing*, Vol. 2, No.1, April 1976.
- Gruber, A., "Estimating rainfall in regions of active convection", *J. Appl. Meteor.*, 12, 1973, pp. 113-118.
- Gupta, S.K., "A distributed digital model for estimation of flows and sediment load from large ungaged watersheds", PhD. Thesis, Department of Civil Engineering, University of Waterloo, Ontario, 1974.

- Holtan, H.N., "A formulation for quantifying the influence of soil porosity and vegetation on infiltration", presented at the 3rd *International Seminar for Hydrology Professors*, Purdue University, Lafayette, Indiana, 1971.
- Holton, J.R., J.M. Wallace and J.A. Young, "On boundary layer dynamics and the ITCZ" in *J. Atmos. Sci.*, 28, 1971, pp. 275-280.
- Howarth, P., "*An evaluation of Landsat imagery for land classification on Eastern Melville Island, N.W.T, Canada*", Ottawa: Environment Canada, 1976.
- Jackson, T.J., R.M. Ragan and R.H. McCuen, "Land-use classification for hydrologic models using interactive machine classification of Landsat data" in *Proceedings of the First Comprehensive Symposium on the Practical Application of Earth Resources Survey Data*, Houston, Texas, 1975, pp. 2365-2378.
- Kesik, A.B., "Analysis of the drainage pattern of selected areas of Canada using ERTS-1 imagery as a base" in *Remote Sensing and Water Resources Management, Proc. 7^o 17*, American Water Resources Association, 1973, pp. 209-224.
- Lacate, D.S., "*Guidelines for Bio-Physical Land Classification*", Publication Nº 1264, Department of Fisheries and Forestry, Canadian Forestry Service, 1969.
- Lauer, D.T., and P.J. Krumpke, "Testing the usefulness of ERTS-1 imagery for inventoring wild land resources in Northern California" in *Proceedings of the Symposium on Significant Results from ERTS-1*, Greenbelt, Maryland, 1973, pp. 97-104.
- Martin, D.W. and V.E. Suomi, "A satellite study of cloud clusters over the tropical North Atlantic Ocean", in *Bull. Amer. Meteor. Soc.*, 53, 1972, pp. 135-156.
- Martin, D.W. and W.D. Sherer, "Review of satellite rainfall estimation methods", in *Bull. Amer. Meteor. Soc.*, 54, 1973, pp. 661-674.
- Meyer, W., and R.I. Welch, "Water Resources Assessment" in *Manual of Remote Sensing*, Robert G. Reeves (ed.), Falls Church, Virginia: American Society of Photogrametry, 1975, pp. 1479-1545.
- Ministerio de Agricultura y Cría, "*Suelos, mapa de órdenes y sub-órdenes, 7a. Aproximación*" (1:500.000), Maracay, 1974.
- Ministerio de Minas e Hidrocarburos, "*Mapa de Hidrología*" (1:500.000), Caracas, 1972.
- Ministerio de Obras Públicas, "*Estudio de suelos: preliminar Biruaca-Apurito, Edo. Apure*", Guanare, 1975.

- Ministerio de Obras Públicas, "*Pluvio-evaporimetría mensual y anual 1971-1974*", Caracas: División de Hidrología, 1975.
- Murray, D.L., "Boughton's daily rainfall-runoff model modified for the Brening Catchment" in *Proceedings of the Symposium on the results of research of representative and experimental basins*, IASH, Pub. 96, N.Z, 1970.
- Myers, V.I., "Crops and Soils" in *Manual of Remote Sensing*, Robert G. Reeves (ed.), Falls Church, Virginia: American Society of Photogrammetry, 1975, pp.1715-1805.
- Ragan, R.M and T.J. Jackson, "Use of satellite data in urban hydrologic models" in *Journal of Hydraulics Division, ASCE*, HY12, 1975, pp. 1469-1475.
- Ragan, R.M. and T.J. Jackson, "*Hydrograph synthesis using Landsat remote sensing and the SCS Models*", Pre-print Nº X-913-76-161, Goodard Space Flight Center, July 1976.
- Rango A., J. Foster and V.V. Salomonson, "Extraction and utilization of space acquired physiographic data for water resources development" in *Remote Sensing and Water Resources Management, American Water Resources Association*, Proc. Nº 17, 1975, pp. 1245-1255.
- Sarmiento, G. and M. Monasterio, "Studies on the savanna vegetation of the Venezuelan Llanos: the use of association analysis" in *Journal of Ecology*, 57, 1969, pp. 579-598.
- Shargel, R. and R.A. González, "*Estudio agrológico preliminar: sectores Bruzual, Mantecal y Anexos*", Caracas: Dirección General de Recursos Hidráulicos, 1973.
- Weik, M.H., "*Standard dictionary of computers and information processing*", Ney York: Hayden, 1969.
- Woodley, W.L. and B. Sancho, "A first step towards rainfall estimation from satellite cloud photographs", *Weather*, 26, 1971, pp. 279-280.

APPENDIX A

LAND-USE/LAND-COVER CLASSIFICATION.

1. *CROPLAND*: land use for annual crops and fallow land.
2. *URBAN-BUILT UP*: includes all built-up areas.
3. *MINES, QUARRIES, SAND AND GRAVEL PITS*: extracting materials areas.
4. *ORCHARD AND VINEYARDS*: fruit trees.
5. *HORTICULTURE, FUR AND POULTRY*: production of vegetables, small fruits, and large scale poultry and fur farming.
6. *ROUGH GRAZING AND RANGELAND*: grasslands (natural); areas of sedges and herbaceous plants; abandoned farmland and lightly wooded grassland.
7. *ROCK AND OTHER UNVEGETATED SURFACES*: areas in which bare surface cover more than 75 % of the total surface.
8. *SWAMP, MARSH OR BOG*: open wetlands, except: areas of swamp grass, and wet land with a dense tree or bush cover.
9. *OUTDOOR RECREATION*: land used either for private or public recreation.
10. *IMPROVED PASTURE AND FORAGE CROPS*: improved pasture only (fodder crops).
11. *SANDS FLATS, DUNES AND BEACHES*.
12. *WOODLAND*: land bearing forest of a commercial nature.

13. *NON-PRODUCTION WOODLAND*: it includes land with a growth of short trees or bushes. Also areas recently logged or burned.
14. *WATER*: permanent bodies of water, large enough to be mapped.

Source: *Gupta (1974)* based on *ARDA*.